

Strong Stability Preservation for Stochastic Partial Differential Equations

J. Woodfield^a

^a*Department of Mathematics, Imperial College London, South Kensington Campus, London, SW7 2AZ, United Kingdom*

Abstract

This paper extends deterministic notions of Strong Stability Preservation (SSP) to the stochastic setting, enabling nonlinearly stable numerical solutions to stochastic differential equations (SDEs) and stochastic partial differential equations (SPDEs) with pathwise solutions that remain unconditionally bounded. This approach may offer modelling advantages in data assimilation, particularly when the signal or data is a realization of an SPDE or PDE with a monotonicity property.

Keywords: SSP, Stochastic, Bounded, Positive, Monotone, Contractive

Contents

1	Introduction	2	
1.1	Motivation	2	
1.2	Literature	2	
1.3	Background: Introduction to deterministic SSP integration.	3	
1.4	Main contributions and outline of the paper.	3	
2	Strong stability preserving stochastic integrators	4	
2.1	Equations	4	
2.2	Well posedness	5	
2.3	Methods	5	
2.4	Convergence	9	
3	Practical Methods and Numerical Demonstrations	15	
3.1	Practical Methods	15	
3.2	Numerical Demonstrations	17	
3.2.1	Example 1a: Stochastic 2D Burgers equation, with slope limiters.	17	
3.2.2	Example 1b: sufficient not necessary	20	
3.2.3	Example 1c: 2D Advection	21	
3.2.4	Example 1d: Incompressible Euler	21	
3.2.5	Example 1e: Operator-Splitting GARK	23	
3.3	Numerical demonstrations with data assimilation	24	
3.3.1	Example 2a: The Twin Experiment, One-dimensional slope limiters	24	
3.3.2	Example 2b: One-dimensional slope limiters, Coarse-grained model reduction.	27	
4	Conclusion	29	
	Appendix A	Appendix	33
	Appendix A.1	Big O notation	33
	Appendix A.2	Multivariate Taylor's theorem	34
	Appendix A.3	Inequalities	34
	Appendix A.4	Particle filter	34

arXiv:2411.11172v1 [math.NA] 17 Nov 2024

1. Introduction

1.1. Motivation

Many important partial differential equations (PDEs) have solutions with monotonic and contractivity properties, typically defined with respect to some convex functional, norm or semi-norm. For example, weak entropy solutions of the one-dimensional Burgers equation are contractive with respect to the total variation semi-norm, $\|u(t^{n+1})\|_{BV(\mathbb{T}^1)} \leq \|u(t^n)\|_{BV(\mathbb{T}^1)}$. Solutions to 2D Euler's equation have bounded vorticity, $\|\omega(t^{n+1})\|_{L^\infty(\mathbb{T}^2)} \leq \|\omega(t^n)\|_{L^\infty(\mathbb{T}^2)}$. The preservation of positivity is a crucially important monotonic property of the advection equation. Furthermore, many different types of monotonicity exist and are of theoretical and practical interest, including local maximum principles, entropy conditions, and contractive behaviour between two solutions $\|q_1(t^{n+1}) - q_2(t^{n+1})\| \leq \|q_1(t^n) - q_2(t^n)\|$. Deterministic Strong Stability Preserving (SSP) methodology was developed to numerically preserve discrete versions of these nonlinear properties.

The solutions to stochastic partial differential equations SPDEs can also have nonlinear properties that are desirable to preserve at a discrete level. SPDEs are an increasingly popular tool used to model physical phenomena that require additional parametrisation. In this paper we investigate strong stability preserving Runge-Kutta methods for stochastic equations, with a focus on constructing unconditionally contractive (monotone) numerical schemes for solving SPDEs. To the best of our knowledge, the stochastic extension/application of SSP time-stepping has not yet been explored. The theory presented here consists of three key components: a spatial scheme that preserves the desired monotone property, a deterministic SSP time-stepping method adapted for the stochastic setting, and appropriately bounded driving increments.

1.2. Literature

Strong stability preserving Runge Kutta (SSPRK) methods are Runge-Kutta methods capable of being written as a convex combination of forward Euler schemes, allowing nonlinear stability properties to be inherited from the forward Euler flow map. The optimal convex combination is referred to as the Shu-Osher [56] representation. It is characterised by a stepsize condition referred to as either the radius of monotonicity or the SSP coefficient. The radius of monotonicity is the largest timestep for which Kraaijevanger's conditions hold [42] and characterises the effectiveness of an RK-scheme to retain monotonic properties.

For a general review of deterministic SSP methods, we refer to the review paper [20] and the references therein. For a selective review of some of the important theoretical developments in the deterministic SSP literature, we refer to [15, 16, 25, 24, 33, 42, 56], where amongst other important developments, the notion of contractivity and the SSP property are unified under different convex functionals. The extension to Additive Runge-Kutta schemes is made in [26] following [42], and then similarly extended to include Generalised Additive Runge-Kutta schemes in [54]. Implicit systems required an extension of the original Shu-Osher representation and is discussed in [5, 57, 16, 25, 24]. To circumnavigate specific order-barriers one can use perturbed RK methods viewed as Additive Runge-Kutta methods in [27, 42]. For large systems, low storage high effective radius of monotonicity methods have been proven effective see [58, 34, 28]. Internal and external monotonicity is discussed in [30]. For an adaptation of the SSP theory to preserve nonlinear properties in the setting of linear operators see [8].

For Stochastic Runge-Kutta methods, convergence to Itô and Stratonovich systems is well established [53, 6, 38, 48] and concepts such as A-Stability have been well developed for both Itô and Stratonovich cases [38]. Whilst SSP theory has not been discussed in the stochastic setting. The related notion of positivity preservation has been studied in the context of SDEs, and we highlight some recent contributions. In [55] positivity preserving theta methods are proposed, using bounded increments is not discussed. In [11] schemes are constructed using the exact solutions of a linearised form of the SDE on short time windows, as to construct positivity-preserving numerical schemes. In [32] a time-adaptive approach is taken, and positivity preservation is discussed in a probabilistic sense. In [36] positivity preservation of a specific SDE is attained through the use of an exponential type integrator. In [23] non-negativity of a Milstein-type scheme is shown in a probabilistic sense. In [4] Stochastic C-stability and B-consistency are established for Milstein-type schemes, what is referred to as satisfying a global monotonicity condition refers to the L2 stability bounds on the drift and diffusion, and not the notion of monotonicity discussed in this paper. More recently in 2023 Fang Zhao and Zhao [13] investigated the SSP property for forward-backwards SDEs for multistep schemes, but defined a notion of strong stability preservation in expectation. Closer to the results and aims as in this paper, [44] show that that

a logarithmic transformed truncated Euler–Maruyama method can attain positive solutions of SDEs with strong order 1/2 convergence. This paper considers strong stability preservation pathwise, and considers schemes with weak convergence order 1 and mean square (strong) order convergence order 1/2.

1.3. Background: Introduction to deterministic SSP integration.

PDEs are often discretised as a system of ordinary differential equations (ODEs), this is common after discretisation in space using the method of lines, where the resulting ODEs take the form

$$\frac{d\mathbf{q}}{dt} = \mathbf{f}(\mathbf{q}), \quad \mathbf{q}(0) = \mathbf{q}_0, \quad \mathbf{q} \in \mathbb{R}^n. \quad (1.1)$$

Strong Stability Preserving (SSP) integrators emerged out of a desire to ensure that numerical methods discretising the system of ODEs satisfy a discrete contractive property analogue to that of the continuum model. One approach commonly taken in the Runge-Kutta framework is to assume that the forward Euler flow map can be proven monotone under an arbitrary convex functional, norm or semi-norm $\|\cdot\|$ for all timesteps less than a critical value τ_0 , i.e. it is assumed

$$\|\mathbf{q}^{n+1}\| = \|\text{FE}(\mathbf{q}^n, \Delta t, \mathbf{f})\| = \|\mathbf{q}^n + \Delta t \mathbf{f}(\mathbf{q}^n)\| \leq \|\mathbf{q}^n\|, \quad \forall \Delta t \leq \tau_0. \quad (1.2)$$

It is then common to write a Runge-Kutta method, as a convex combination of forward Euler steps. For example, the Heun scheme admits the following representation

$$\text{Heun}(\mathbf{q}^n, \Delta t, \mathbf{f}) = 1/2 \mathbf{q}^n + 1/2 \text{FE}(\text{FE}(\mathbf{q}^n, \Delta t, \mathbf{f}), \Delta t, \mathbf{f}). \quad (1.3)$$

Since it is assumed proven for forward Euler, one can show that using the convex combination representation, the same monotone property holds for the HEUN scheme as follows

$$\|\mathbf{q}^{n+1}\| = \|\text{Heun}(\mathbf{q}^n, \Delta t, \mathbf{f})\| \leq 1/2 \|\mathbf{q}^n\| + 1/2 \|\text{FE}(\text{FE}(\mathbf{q}^n, \Delta t, \mathbf{f}), \Delta t, \mathbf{f})\| \leq \|\mathbf{q}^n\|, \quad \forall \Delta t \leq \tau_0. \quad (1.4)$$

In this paper, we note that the notion of strong stability can be extended into the stochastic setting for some widely used stochastic integrators. More specifically we formalise and generalise an argument of the following form. Should the Euler-Maruyama map be SSP in the following sense $\|\text{EM}(\mathbf{q}^n, \Delta t, \mathbf{f}, G, \Delta \mathbf{W})\| \leq \|\mathbf{q}^n\|$ (requiring bounded increments). Then a stochastic Heun scheme with a particular convex representation can be bounded as follows

$$\|\mathbf{q}^{n+1}\| = \|\text{Stochastic-Heun}(\mathbf{q}^n, \Delta t, \mathbf{f}, G, \Delta \mathbf{W})\| \leq 1/2 \|\mathbf{q}^n\| + 1/2 \|\text{EM}^2(\mathbf{q}^n, \Delta t, \mathbf{f}, G, \Delta \mathbf{W})\| \leq \|\mathbf{q}^n\|, \quad (1.5)$$

and could inherit nonlinear monotonic properties from the Euler Maruyama scheme.

1.4. Main contributions and outline of the paper.

In this work, we establish that three conditions are required for a stochastic Runge-Kutta scheme to be SSP.

1. A provably monotonic numerical method for the Euler Maruyama scheme.
2. Bounded increments.
3. The application of an SSP-RK scheme with a nonzero radius of monotonicity.

Where condition 2 is required for condition 1. The extension to Additive Runge-Kutta schemes and Generalised Additive Runge-Kutta schemes is also considered, allowing condition 1 to be relaxed to the following strictly weaker condition. One requires a provably monotonic numerical method for the Forward Euler scheme and a drift-only Euler Maruyama scheme.

In section 2 we define what it means for some stochastic RK, ARK and GARK schemes to be SSP. Methods of proofs follow the deterministic literature [42, 25], but are applied in the stochastic setting. In section 2.4 we discuss the convergence implications of using bounded increments. More specifically we prove a variant of a theorem stated by Milstein and Tretyakov [49, 50], where normal increments can be truncated and one can still attain strong order of convergence. The outline of proof is sketched in [49] and an in-depth derivation is

provided for the backward Euler Maruyama scheme is found in [49]. Whilst this result is known, a detailed proof for the Additive Runge-Kutta method involving regularity conditions has been omitted in the literature. In section 3.1 we introduce some practical methods. In section 3.2.1, we demonstrate all three conditions are of practical value to creating a monotonic solution. In section 3.2.2, we numerically demonstrate that these conditions may not be strictly necessary. In section 3.2.3 we show that when using multidimensional slope limiters with SSP integration with bounded increments it is possible to produce range-bounded solutions to a stochastic advection equation. In section 3.2.4 we show one-dimensional slope limiters can be used with an SSP method with bounded increments to produce range-bounded solutions to Euler’s equation with transport-type noise. In section 3.2.5, we illustrate that when an EM scheme may not be proven monotone one can employ SARK and SGARK methods to construct bounded solutions to a Burgers equation with deformational spatially varying transport noise.

In section 3.3.1 we produce ensemble solutions to a 1d stochastic compressible advection equation with and without a particle filter and compute ensemble forecast metrics when the data is a realisation of the monotone forward model. In section 3.3.2 we perform the same experiment, however, we no longer use idealised data but generate reference data from a higher resolution PDE with a similar monotonic property. We show an increase in continuous ranked probability score when using SSP methodology with slope limiting as a function of lead time, indicating potential modelling advantages.

2. Strong stability preserving stochastic integrators

2.1. Equations

We consider the d -dimensional stochastic process $\mathbf{q}(t)$, defined as the solution of the Stratonovich SDE

$$\mathbf{q}(t) = \mathbf{q}(0) + \int_0^t \mathbf{f}(\mathbf{q})ds + \sum_{p=1}^P \int_0^t \mathbf{g}_p(\mathbf{q}) \circ dW_s^p; \quad \mathbf{q}(0) = \mathbf{q}_0. \quad (2.1)$$

over $[0, t]$ for some $t \in \mathbb{R}^{>0}$. Here the initial state is denoted $\mathbf{q}_0 \in \mathbb{R}^d$ at $t_0 = 0$, the vector valued drift function is denoted $\mathbf{f}(\mathbf{q}) : \mathbb{R}^d \rightarrow \mathbb{R}^d$, the matrix valued diffusion is denoted $G(\mathbf{q}) : \mathbb{R}^d \rightarrow \mathbb{R}^{d \times P}$ whose p th column is denoted $\mathbf{g}_p(\mathbf{q}) : \mathbb{R}^d \rightarrow \mathbb{R}^d$ for $p = \{1, \dots, P\}$. Finally, we denote a P -dimensional \mathcal{F}_t -adapted real-valued vector Wiener process as $(\mathbf{W}_t)_{t \geq 0} = ((W_t^1, \dots, W_t^P)^T)_{t \geq 0}$, such that the components are scalar adapted independent Wiener processes taking values on a filtered probability space $(\Omega, \mathcal{F}, \mathbb{P}; (\mathcal{F}_t)_{t \geq 0})$ with the usual conditions¹. The \circ denotes Stratonovich integration. These d -dimensional systems often arise after the spatial discretisation of stochastic partial differential equations in the method of lines framework. System eq. (2.1) can be denoted with the following “differential” shorthand

$$d\mathbf{q} = \mathbf{f}(\mathbf{q})dt + G(\mathbf{q}) \circ d\mathbf{W}(t). \quad (2.2)$$

We shall also refer to the following Itô system

$$\mathbf{q}^I(t) = \mathbf{q}^I(0) + \int_0^t \mathbf{f}(\mathbf{q}^I)ds + \sum_{p=1}^P \int_0^t \mathbf{g}_p(\mathbf{q}^I)dW_s^p; \quad \mathbf{q}^I(0) = \mathbf{q}_0. \quad (2.3)$$

An SDE, whose stochastic integration is understood in the Itô sense [51, 31], whose shorthand is

$$d\mathbf{q}^I = \mathbf{f}(\mathbf{q}^I)dt + G(\mathbf{q}^I)d\mathbf{W}_t. \quad (2.4)$$

The Stratonovich SDE eq. (2.1) can be written as an Itô SDE with a modified drift

$$\mathbf{q}(t) = \mathbf{q}(0) + \int_0^t \underline{\mathbf{f}}(\mathbf{q})ds + \sum_{p=1}^P \int_0^t \mathbf{g}_p(\mathbf{q})dW_s^p; \quad \mathbf{q}(0) = \mathbf{q}_0, \quad (2.5)$$

whose drift differs by the Itô Stratonovich correction.

¹The usual conditions for a filtered probability space. The filtration (a collection of increasing sub σ -algebras of \mathcal{F}) is assumed right continuous (in the sense that $\mathcal{F}_t = \{A \in \mathcal{F}_0 : A \in \mathcal{F}_s, \forall s > t\}$) the measure space $(\Omega, \mathcal{F}, \mathbb{P})$ is assumed complete, and it is also assumed that if $\mathbb{P}(A) = 0$, then $A \in \mathcal{F}_0$ (see [46, 51]).

2.2. Well posedness

The existence and uniqueness of the Stratonovich ODE system is well known and requires Lipschitz continuity and linear growth bounds on the Itô Stratonovich corrected drift and diffusion. These are expressed below, where we have used L to define an arbitrary constant

$$\|\underline{\mathbf{f}}(\mathbf{q})\|_2^2 \leq L(1 + \|\mathbf{q}\|_2^2), \quad \|G(\mathbf{q})\|_F^2 \leq L(1 + \|\mathbf{q}\|_2^2), \quad \forall \mathbf{q} \in \mathbb{R}^d, \quad (2.6)$$

$$\|\underline{\mathbf{f}}(\mathbf{q}_1) - \underline{\mathbf{f}}(\mathbf{q}_2)\|_2 \leq L\|\mathbf{q}_1 - \mathbf{q}_2\|_2, \quad \|G(\mathbf{q}_1) - G(\mathbf{q}_2)\|_F \leq L\|\mathbf{q}_1 - \mathbf{q}_2\|_2, \quad \forall \mathbf{q}_1, \mathbf{q}_2 \in \mathbb{R}^d. \quad (2.7)$$

Whereas the Itô system requires the same conditions but for the uncorrected drift \mathbf{f} (permitting lower regularity on G). In [46], the existence and uniqueness of the Itô system is established using the contraction mapping theorem in the Banach space $(\mathcal{H}_{2,T}, \|\cdot\|_{\mathcal{H}_{2,T}})$, the set of \mathbb{R}^d -valued predictable processes $\{\mathbf{q}(t) : t \in [0, T]\}$ such that $\|\mathbf{q}\|_{\mathcal{H}_{2,T}} := \sup_{t \in [0, T]} \mathbb{E}[\|\mathbf{q}(t)\|_2^2]^{1/2} < \infty$. Existence and pathwise uniqueness of strong solutions is also established in [39] under the assumptions of joint measurability of both diffusion and drift, initially bounded moments and the Lipschitz and linear growth bounds (page 128 [39]). However, rather than bounding the Frobenius norm they (equivalently) require that

$$\|\mathbf{g}_p\|_2^2 \leq L(1 + \|\mathbf{q}\|_2^2), \quad \|\mathbf{g}_p(\mathbf{q}_1) - \mathbf{g}_p(\mathbf{q}_2)\|_2^2 \leq L\|\mathbf{q}_1 - \mathbf{q}_2\|_2^2, \quad \forall p \in \{1, \dots, P\}. \quad (2.8)$$

Some of these inequalities are used later in this paper when establishing estimates required for the Fundamental theorem of mean square convergence [49].

2.3. Methods

Similar in analogy to how the deterministic SSP literature builds schemes in terms of the forward Euler flow map, we will discuss particular stochastic Runge-Kutta methods built upon convex combinations of the Euler Maruyama scheme defined below.

Method 2.1 (Euler-Maruyama). The Euler-Maruyama scheme is a numerical flow map

$EM(\mathbf{q}^n, \Delta t, \mathbf{f}, G, \Delta \mathbf{S}) : \mathbf{q}^n \in \mathbb{R}^d \rightarrow \mathbf{q}^{n+1} \in \mathbb{R}^d$, advancing the current state variable \mathbf{q}^n by a increment of time $\Delta t \in \mathbb{R}^{>0}$, as follows

$$\mathbf{q}^{n+1} = \mathbf{q}^n + \mathbf{f}(\mathbf{q}^n)\Delta t + G(\mathbf{q}^n)\Delta \mathbf{S}, \quad (2.9)$$

where $\Delta \mathbf{S}$ is a realisation of a P dimensional signal (typically drawn from a distribution) and $G(\mathbf{q})\Delta \mathbf{S}$, is understood as a matrix vector product $(\mathbb{R}^{d \times P}, \mathbb{R}^P) \rightarrow \mathbb{R}^d$, defined by $G(\mathbf{q})\Delta \mathbf{S} = \sum_{p=1}^{p=P} \mathbf{g}_p(\mathbf{q}^n)\Delta S^p$.

Typically, in the context of Brownian motion $\Delta W^p = \int_{t^n}^{t^{n+1}} dW^p(s) = W^p(t^{n+1}) - W^p(t^n) \sim \sqrt{\Delta t}N(0, 1)$, one samples from a scaled normally distribution, and one can establish convergence to the Itô equation eq. (2.3). However, this is not a necessary condition for either weak or strong convergence of the numerical scheme. Sampling from random variables with bounded increments will be essential for the theoretical developments in this paper and allows us to define (in definition 2.1) an EM scheme with an SSP property. We postpone how using bounded increments affects the convergence until later in section 2.4.

Definition 2.1 (Strong Stability Preservation of Euler-Maruyama scheme.). The Euler-Maruyama scheme, will be defined to be SSP with respect to the arbitrary convex semi-norm $\|\cdot\|$, if there exists a critical timestep $\tau_0 \geq 0$, such that for all positive timesteps smaller than this $\forall \Delta t \in (0, \tau_0)$ and for all possible sampled increments ΔS^p . The following property holds

$$\|\mathbf{q}^{n+1}\| = \|\mathbf{q}^n + \mathbf{f}(\mathbf{q}^n)\Delta t + \sum_{p=1}^P \mathbf{g}_p(\mathbf{q}^n)\Delta S^p\| \leq \|\mathbf{q}^n\|. \quad (2.10)$$

This particular definition requires ΔS^p , to be bounded.

We now consider a particular Stochastic Runge-Kutta method 2.2 and subsequently define an SSP property (definition 2.2).

Method 2.2 (Stochastic Runge-Kutta). An s -stage Stochastic RK method is defined by the Butcher Tableau $A \in \mathbb{R}^{s \times s}$, $b \in \mathbb{R}^s$. Such that the old value \mathbf{q}^n is updated by the use of s internal substages k^i as follows

$$\mathbf{q}^{n+1} = \mathbf{q}^n + \Delta t \sum_{i=1}^s b_i \mathbf{f}(\mathbf{k}^i) + \sum_{i=1}^s b_i G(\mathbf{k}^i) \Delta \mathbf{S}, \quad \text{where} \quad \mathbf{k}^i = \mathbf{q}^n + \Delta t \sum_{j=1}^s a_{ij} \mathbf{f}(\mathbf{k}^j) + \sum_{j=1}^s a_{ij} G(\mathbf{k}^j) \Delta \mathbf{S}. \quad (2.11)$$

The increments $\Delta \mathbf{S}$ are sampled once at t^n , and contracted against the diffusion matrix G , such that the same increments are reused at different sub-stages of the RK method.

Definition 2.2 (SSP-SRK). The Stochastic Runge-Kutta method 2.2 is said to be strong stability preserving with a radius of monotonicity C if the numerical solution \mathbf{q}^{n+1} generated by the numerical method in eq. (2.11) satisfies the following property

$$\|\mathbf{q}^{n+1}\| \leq \|\mathbf{q}^n\|, \quad \forall \Delta t \leq C\tau_0, \quad \forall \Delta \mathbf{S}_i^p. \quad (2.12)$$

Where it is assumed that there exists a critical timestep τ_0 such that the Euler Maruyama scheme is SSP as specified in definition 2.1. Method 2.2 is said to be internally strong stability preserving with radius of monotonicity C when the substages satisfy $\|\mathbf{q}^{n+1}\| \leq \|\mathbf{k}^i\| \leq \|\mathbf{k}^{i-1}\| \leq \|\mathbf{q}^n\|$, for all $\Delta t \leq C\tau_0$, for all sampled increments $\Delta \mathbf{S}$, for all $i \in \{1, \dots, s\}$.

Remark. The convex combination (Shu-Osher) representation of a Runge-Kutta method enables the preservation of monotonic properties that are strictly stronger than contractivity for any convex functional. For example, the Shu-Osher representation allows the enforcement of local maximum principles at each substage in a Runge Kutta method.

Throughout this work we will adopt the compact notation from [25], where a butcher tableau (A, \mathbf{b}) is turned into the following matrix

$$\mathbb{A} = \begin{pmatrix} A & 0 \\ \mathbf{b}^T & 0 \end{pmatrix} \in \mathbb{R}^{(s+1) \times (s+1)}. \quad (2.13)$$

Theorem 2.1 (Stochastic Runge-Kutta method 2.2 is SSP with radius of monotonicity $R(\mathbb{A})$). Assuming there exists a critical timestep τ_0 such that EM is assumed contractive with respect to a convex functional, then method 2.2 is also contractive with respect to the same convex functional with timestep condition $\Delta t \leq R(\mathbb{A})\tau_0$, where

$$R(\mathbb{A}) = \max\{r \mid r \geq 0; \forall s \in [0, r], (I + s\mathbb{A}) \in \text{GL}(s+1, \mathbb{R}), (I + s\mathbb{A})^{-1} s\mathbb{A} \geq 0, (I + s\mathbb{A})^{-1} \mathbf{e}_s \geq 0\}. \quad (2.14)$$

The conditions in eq. (2.14) are algebraically equivalent to the Kraaijevanger [42] conditions [25, 24] on the butcher tableau (A, \mathbf{b}) , namely $I + sA$ is nonsingular, and $1 + sb^T(I + sA)^{-1} \mathbf{e}_s \geq 0$, $A(I + sA)^{-1} \geq 0$, $b^T(I + sA)^{-1} \geq 0$, and $(I + sA)^{-1} \mathbf{e}_s \geq 0$.

Proof. By identifying the vector-valued function $\mathfrak{F}(\mathbf{q}) : \mathbb{R}^n \mapsto \mathbb{R}^n$ associated with

$$\mathfrak{F}(\mathbf{q}) := \mathbf{f}(\mathbf{q}^n) + G(\mathbf{q}^n) \Delta \mathbf{S} (\Delta t)^{-1}, \quad (2.15)$$

one can make an equivalence between the Euler Maruyama Scheme, and the forward Euler scheme as follows

$$FE(\mathbf{q}^n, \Delta t, \mathfrak{F}) = \mathbf{q}^n + \Delta t \mathfrak{F}(\mathbf{q}^n) = \text{EM}(\mathbf{q}^n, \Delta t, \mathbf{f}, G, \Delta \mathbf{S}). \quad (2.16)$$

Furthermore, this same identification allows the stochastic Runge-Kutta method 2.2, to be defined by a single s -stage RK method defined by a real matrix $A \in \mathbb{R}^{s \times s}$, and a real vector $b \in \mathbb{R}^s$. Such that the old value \mathbf{q}^n is updated by the use of s internal substages k^i as follows

$$\mathbf{q}^{n+1} = \mathbf{q}^n + \Delta t \sum_{i=1}^s b_i \mathfrak{F}(\mathbf{k}^i) \quad \text{where} \quad \mathbf{k}^i = \mathbf{q}^n + \Delta t \sum_{j=1}^s a_{ij} \mathfrak{F}(\mathbf{k}^j) \quad \forall i \in \{1, \dots, s\}. \quad (2.17)$$

These identifications, allow the entire deterministic SSPRK theory to be directly translated into the setting of stochastic Runge-Kutta methods. The method of proof can then follow one established in the deterministic literature (see [42, 25, 20]), repeated here for clarity and self-containedness. Add $r \sum_{j=1}^s a_{ij} \mathbf{k}^j$, to both the LHS and RHS of the substage equation for \mathbf{k}^i , and add $r \sum_{j=1}^s b_j \mathbf{k}^j$ to both sides of the equation for the final stage \mathbf{q}^{n+1} in eq. (2.17) to give

$$\mathbf{k}^i + r \sum_{j=1}^s a_{ij} \mathbf{k}^j = \mathbf{q}^n + r \sum_{j=1}^s a_{ij} \mathbf{k}^j + \Delta t \sum_{j=1}^s a_{ij} \mathfrak{F}(\mathbf{k}^j), \quad \forall i \in \{1, \dots, s\}, \quad (2.18)$$

$$\mathbf{q}^{n+1} + r \sum_{j=1}^s b_j \mathbf{k}^j = \mathbf{q}^n + r \sum_{j=1}^s b_j \mathbf{k}^j + \Delta t \sum_{j=1}^s b_j \mathfrak{F}(\mathbf{k}^j). \quad (2.19)$$

This allows the scheme to be written in terms of Euler Maruyama flow maps as follows

$$\mathbf{k}^i + r \sum_{j=1}^s a_{ij} \mathbf{k}^j = \mathbf{q}^n + r \sum_{j=1}^s a_{ij} \text{EM}(\mathbf{k}^j, \Delta t/r, \mathbf{f}, G, \Delta S/r^{1/2}), \quad \forall i \in \{1, \dots, s\}, \quad (2.20)$$

$$\mathbf{q}^{n+1} + r \sum_{j=1}^s b_j \mathbf{k}^j = \mathbf{q}^n + r \sum_{j=1}^s b_j \text{EM}(\mathbf{k}^j, \Delta t/r, \mathbf{f}, G, \Delta S/r^{1/2}). \quad (2.21)$$

In the instance of a one dimensional SDE when $d = 1$, one can write eqs. (2.20) and (2.21) as

$$(I + r\mathbb{A})\mathbf{S} = \mathbf{q}^n \mathbf{e}_{s+1} + r\mathbb{A} \text{EM}(\mathbf{S}). \quad (2.22)$$

This is a convex combination under the conditions, $(I + r\mathbb{A})^{-1}r\mathbb{A} > 0$, $(I + r\mathbb{A})^{-1}\mathbf{e}_{s+1} > 0$, since these matrices add to give the identity matrix. For $d > 1$, one can employ the notation in [25], which conveniently extends the theory to vector-valued ODEs (and SDEs). We let $\mathbf{S} := ((\mathbf{k}^1)^T, \dots, (\mathbf{k}^s)^T, (\mathbf{q}^{n+1})^T)^T \in \mathbb{R}^{(s+1)d}$ be a vector containing the sub-stages and the final stage. We let

$$\text{EM}(\mathbf{S}) := (\text{EM}(\mathbf{k}^1)^T, \text{EM}(\mathbf{k}^1)^T, \dots, \text{EM}(\mathbf{k}^n)^T, 0\mathbf{e}_d^T)^T. \quad (2.23)$$

Then eqs. (2.20) and (2.21) is written as

$$\mathbf{S} + (\mathbb{A} \otimes_{\text{Kron}} I)\mathbf{S} = \mathbf{e}_{s+1} \otimes_{\text{Kron}} \mathbf{q}^n + r(\mathbb{A} \otimes_{\text{Kron}} I) \text{EM}(\mathbf{S}), \quad (2.24)$$

where $\mathbb{A} \otimes_{\text{Kron}} I \in \mathbb{R}^{(s+1)d \times (s+1)d}$. So as before, a convex combination can be achieved below

$$\mathbf{S} = (I_{(s+1)d} + (\mathbb{A} \otimes_{\text{Kron}} I))^{-1}(\mathbf{e} \otimes_{\text{Kron}} \mathbf{q}^n) + (I + (\mathbb{A} \otimes_{\text{Kron}} I))^{-1}r(\mathbb{A} \otimes_{\text{Kron}} I) \text{EM}(\mathbf{S}) \quad (2.25)$$

under the manipulation of the Kronecker product, the same Kraijevanger conditions are observed. \square

We will discuss the strong stability preservation of a particular Stochastic Additive Runge-Kutta (SARK) method built upon convex combinations of a diffusion-only Euler Maruyama scheme and a deterministic forward Euler scheme.

Method 2.3 (Stochastic Additive Runge-Kutta). We define the Stochastic Additive Runge-Kutta flow map associated with treating the drift \mathbf{f} and diffusion G with the Butcher tableaux (A, b) , (\tilde{A}, \tilde{b}) respectively by

$$\mathbf{q}^{n+1} = \mathbf{q}^n + \Delta t \sum_{i=1}^s b_i \mathbf{f}(\mathbf{k}^i) + \sum_{i=1}^s \tilde{b}_i G(\mathbf{k}^i) \Delta \mathbf{S}, \quad \text{where} \quad \mathbf{k}^i = \mathbf{q}^n + \Delta t \sum_{j=1}^s a_{i,j} \mathbf{f}(\mathbf{k}^j) + \sum_{j=1}^s \tilde{a}_{i,j} G(\mathbf{k}^j) \Delta \mathbf{S}. \quad (2.26)$$

Where $i \in \{1, \dots, s\}$, and as before $G\Delta S$ denotes a matrix vector product.

The SARK method is a strict generalisation of the previous SRK method, allowing the drift to be treated with a different Butcher-Tableau than the diffusion. The Stochastic Additive Runge-Kutta method inherits monotonic properties from both the FE flow map and the EM without drift flow map, a specific consequence of choosing this particular additive structure. This is particularly useful if the Euler Maruyama scheme cannot be proven monotone in the presence of both drift and diffusion.

Theorem 2.2 (Stochastic Additive Runge-Kutta method 2.3 is SSP under the usual ARK extension of the Kraaijevanger conditions.). It is assumed that one can establish the following properties,

$$\|\mathbf{q}^n + \Delta t \mathbf{f}(\mathbf{q}^n)\| \leq \|\mathbf{q}^n\|, \quad \forall \Delta t \leq \tau_f, \quad (2.27)$$

$$\|\mathbf{q}^n + G(\mathbf{q}^n) \Delta \mathbf{S}\| \leq \|\mathbf{q}^n\|, \quad \forall \Delta t \leq \tau_g, \quad \forall \Delta \mathbf{S}. \quad (2.28)$$

Then if $\Delta t \leq \tau_f r$ and $\Delta t \leq \tau_g \tilde{r}$, $\forall (r, \tilde{r}) \in \mathcal{R}(\mathbb{A}, \tilde{\mathbb{A}})$ then method 2.3 preserves the desired notion of nonlinear stability. The region of absolute monotonicity, denoted by $\mathcal{R}(\mathbb{A}, \tilde{\mathbb{A}})$, is defined by the set of positive values (r, \tilde{r}) in which the natural extension of Kraaijevangers conditions [25, 42] hold

$$I + r\mathbb{A} + \tilde{r}\tilde{\mathbb{A}} \in GL(s+1, \mathbb{R}), \quad (2.29)$$

$$(I + r\mathbb{A} + \tilde{r}\tilde{\mathbb{A}})^{-1} \mathbb{A} \geq 0, \quad (2.30)$$

$$(I + r\mathbb{A} + \tilde{r}\tilde{\mathbb{A}})^{-1} \tilde{\mathbb{A}} \geq 0, \quad (2.31)$$

$$(I + r\mathbb{A} + \tilde{r}\tilde{\mathbb{A}})^{-1} \mathbf{e} \geq 0. \quad (2.32)$$

Where the inequalities are understood point-wise, and if the set $\mathcal{R}(\mathbb{A}, \tilde{\mathbb{A}})$ has measure 0, the ARK method is not SSP and has no region of absolute monotonicity.

Proof. We identify the following FE, and diffusion EM flow maps,

$$\text{FE}(\mathbf{q}, \Delta t, \mathbf{f}) = \mathbf{q}^n + \Delta t \mathbf{f}(\mathbf{q}^n), \quad \text{EM}(\mathbf{q}, \Delta \mathbf{S}, G) = \mathbf{q}^n + \Delta t \sum_{p=1}^P (\Delta t)^{-1} \mathbf{g}_p(\mathbf{q}^n) \Delta \mathbf{S}^p, \quad (2.33)$$

each assumed to be SSP under the critical timestep condition τ_f, τ_G respectively eqs. (2.27) and (2.28). Then the SARK method 2.3 is decomposable in the way deterministic Additive RK methods are ([42, 25]), using the notation $\mathbb{A}, \tilde{\mathbb{A}}$ allows the following compact representation,

$$\mathbf{S} = \mathbf{e}_{s+1} \otimes_{kron} \mathbf{q}^n + \Delta t (\mathbb{A} \otimes_{kron} I) \mathbf{F}(\mathbf{S}) + \Delta t (\tilde{\mathbb{A}} \otimes_{kron} I) \mathcal{G}(\mathbf{S}). \quad (2.34)$$

Where

$$\mathbf{e} = (1, \dots, 1)^T \in \mathbb{R}^{s+1}, \quad \mathbf{S} = ((\mathbf{k}^1)^T, \dots, (\mathbf{k}_s)^T, \mathbf{q}_{n+1}^T)^T \in \mathbb{R}^{(s+1)d}, \quad (2.35)$$

$$\mathbf{F}(\mathbf{S}) = \left(\mathbf{f}(\mathbf{k}^1)^T, \dots, \mathbf{f}(\mathbf{k}^s)^T, 0 \right)^T \in \mathbb{R}^{(s+1)d}, \quad (2.36)$$

$$\mathcal{G}(\mathbf{S}) = \Delta t^{-1} \left(\left(\sum_{p=1}^P \mathbf{g}_p(\mathbf{k}^1) \Delta \mathbf{S}^p \right)^T, \dots, \left(\sum_{p=1}^P \mathbf{g}_p(\mathbf{k}^s) \Delta \mathbf{S}^p \right)^T, 0 \right)^T \in \mathbb{R}^{(s+1)d}. \quad (2.37)$$

The symbol \otimes_{kron} denotes the Kronecker product. Let $d = 1$ such that we can consider

$$\mathbf{S} = q^n \mathbf{e}_{s+1} + \Delta t \mathbb{A} \mathbf{F}(\mathbf{S}) + \Delta t \tilde{\mathbb{A}} \mathcal{G}(\mathbf{S}) \quad (2.38)$$

We add $r\mathbb{A}\mathbf{S}$ and $\tilde{r}\tilde{\mathbb{A}}\mathbf{S}$ to both sides of eq. (2.38), to give

$$\mathbf{S} + r\mathbb{A}\mathbf{S} + \tilde{r}\tilde{\mathbb{A}}\mathbf{S} = q^n \mathbf{e}_{s+1} + r\mathbb{A} \left(\mathbf{S} + \frac{\Delta t}{r} \mathbf{F}(\mathbf{S}) \right) + \tilde{r}\tilde{\mathbb{A}} \left(\mathbf{S} + \frac{\Delta t}{\tilde{r}} \mathcal{G}(\mathbf{S}) \right). \quad (2.39)$$

We now define, $M = I + r\mathbb{A}\mathbf{S} + \tilde{r}\tilde{\mathbb{A}}\mathbf{S}$, such that we have

$$\mathbf{S} = M^{-1} q^n \mathbf{e}_{s+1} + r M^{-1} \mathbb{A} \left(\mathbf{S} + \frac{\Delta t}{r} \mathbf{F}(\mathbf{S}) \right) + \tilde{r} M^{-1} \tilde{\mathbb{A}} \left(\mathbf{S} + \frac{\Delta t}{\tilde{r}} \mathcal{G}(\mathbf{S}) \right). \quad (2.40)$$

Suppose that the following conditions hold (natural extension of Kraaijevanger conditions)

$$M := I + r\mathbb{A}\mathbf{S} + \tilde{r}\tilde{\mathbb{A}}\mathbf{S} \in GL(\mathbb{R}^{s+1}), \quad M^{-1} \mathbf{e} \geq 0, \quad M^{-1} \mathbb{A} \geq 0, \quad M^{-1} \tilde{\mathbb{A}} \geq 0. \quad (2.41)$$

Since $M^{-1} + M^{-1} r\mathbb{A} + M^{-1} \tilde{r}\tilde{\mathbb{A}} = M^{-1} (I + r\mathbb{A} + \tilde{r}\tilde{\mathbb{A}}) = M M^{-1} = I$, then eq. (2.40) is a convex combination. With $\Delta t \leq \min(r\tau_f, \tilde{r}\tau_g)$ one attains monotonicity of the stochastic additive Runge-Kutta scheme. The higher dimensional case when $d \geq 1$, follows analogously under standard manipulations of the Kronecker product \otimes_{kron} , see [25]. \square

We define a particular Generalised Additive Runge-Kutta (GARK) method for stochastic schemes as follows.

Method 2.4 (Stochastic Generalised Additive Runge-Kutta). We define the Stochastic Generalised Additive Runge-Kutta flow map as follows

$$\mathbf{k}_i^f = \mathbf{q}^n + \Delta t \sum_{j=1}^{s^f} a_{i,j}^{f,f} \mathbf{f}(\mathbf{k}_j^f) + \sum_{j=1}^{s^g} a_{i,j}^{f,g} G(\mathbf{k}_j^g) \Delta \mathbf{S}, \quad i \in \{1, \dots, s^f\}, \quad (2.42)$$

$$\mathbf{k}_i^g = \mathbf{q}^n + \Delta t \sum_{j=1}^{s^f} a_{i,j}^{g,f} \mathbf{f}(\mathbf{k}_j^f) + \sum_{j=1}^{s^g} a_{i,j}^{g,g} G(\mathbf{k}_j^g) \Delta \mathbf{S}, \quad i \in \{1, \dots, s^g\}, \quad (2.43)$$

$$\mathbf{q}^{n+1} = \mathbf{q}^n + \Delta t \sum_{i=1}^{s^f} b_i^f \mathbf{f}(\mathbf{k}_i^f) + \sum_{i=1}^{s^g} b_i^g G(\mathbf{k}_i^g) \Delta \mathbf{S}. \quad (2.44)$$

GARK schemes allow different stage values for different components.

The extension of the SSP theory to stochastic systems can be made using the theory developed in [54], whilst making associations to appropriate FE maps similar to the previous examples in this paper. Rather than elaborate on such a construction, we shall instead introduce some practical examples (method 3.5, method 3.4) based on operator splitting later in this paper.

2.4. Convergence

One requires having bounded increments for the stochastic generalisation of the SSP property. One approach to having bounded increments is to sample from bounded distributions agreeing in moments with the normal distribution. Two classical methods are as follows.

Example 2.1. The P -dimensional random variable whose components are two-point random variables

$$\mathbb{P} \left(\Delta \widetilde{W}^p = \pm \sqrt{\Delta t} \right) = 1/2, \quad (2.45)$$

has the same first 3 moments as that of the $N(0, \Delta t)$ distribution and satisfies $|\mathbb{E}[\widetilde{W}]| + |\mathbb{E}[\widetilde{W}^3]| + |\mathbb{E}[\widetilde{W}^2] - \Delta t| \leq K \Delta t^2$ sufficient for weak order 1 of convergence [38].

Example 2.2. Also found in [38] the P dimensional random variable defined component-wise as a three-point random variable

$$\mathbb{P} \left(\Delta \widetilde{W}^p = \pm \sqrt{3\Delta t} \right) = 1/6, \quad \mathbb{P} \left(\Delta \widetilde{W}^p = 0 \right) = 2/3, \quad (2.46)$$

is a distribution with the same first 5 moments as that of the normal $N(0, \Delta t)$ distribution and satisfies a similar moment estimate $|\mathbb{E}[\widetilde{W}]| + |\mathbb{E}[\widetilde{W}^2] - \Delta t| + |\mathbb{E}[\widetilde{W}^3]| + |\mathbb{E}[\widetilde{W}^4] - 3\Delta t| + |\mathbb{E}[\widetilde{W}^5]| \leq K \Delta t^3$.

Whilst one can retain the weak order of convergence (sufficient for most applications) provided high enough moments are captured and the drift and diffusion are sufficiently differentiable [38], one can lose the strong order of convergence or the mean square order of convergence by sampling from such distributions. The remainder of this section discusses strong and mean square convergence when cutting the tails of the normal distribution and can be avoided for those who wish to have weak convergence. The mean square order of convergence is defined below in definition 2.3.

Definition 2.3 (Mean square convergence). The output of a numerical method \mathbf{q}^n converges in the mean-square sense with order $p > 0$ to the exact solution $\mathbf{q}(t^n)$ of an SDE at time t^n if there exists a constant $L > 0$, and a critical timestep $\tau_c > 0$ such that for each $\Delta t \in (0, \tau_c]$, on has

$$\left(\mathbb{E} \left[\|\mathbf{q}^n - \mathbf{q}(t_n)\|_2^2 \right] \right)^{1/2} \leq L \Delta t^p. \quad (2.47)$$

Strong convergence is defined below.

Definition 2.4 (Strong global convergence). Let \mathbf{q}^n denote the numerical approximation of the stochastic process \mathbf{q} at time t^n , after n steps of equal step-size Δt . We say that the numerical method is converging with strong global order p if $\exists \tau_c > 0, L > 0$, s.t $\mathbb{E}[\|\mathbf{q}^n - \mathbf{q}(t^n)\|_2] \leq L\Delta t^p, \quad \forall \Delta t \in (0, \tau_c)$.

Mean square convergence implies strong convergence under Lyapunov's inequality. To retain the mean square (strong) order of the scheme whilst using bounded increments, one can truncate the tails of the normal distribution. More specifically in [49] the increments in eq. (2.48) were proven to converge to the Itô system when using a Backward Euler discretisation. As is common, the increments $\Delta W \sim N(0, \Delta t)$ can be written in terms of the standard normal distribution $\Delta Z \sim N(0, 1)$, by rescaling $\Delta W = \sqrt{\Delta t}\Delta Z$. Similarly, the bounded increments in eq. (2.48) can be rescaled as $\Delta \tilde{W} = \sqrt{\Delta t}\Delta \tilde{Z}$.

Definition 2.5 (Milstein-Tretyakov Bounded normal increments). Given $\Delta Z \sim N(0, 1)$ and $\Delta t \in \mathbb{R}^{>0}$, Milstein and Tretyakov [50] define a symmetric bounded increment $\Delta \tilde{Z}_{\Delta t}$, from the following random variable,

$$\Delta \tilde{Z}_{\Delta t} := \begin{cases} \Delta Z, & |\Delta Z| \leq A_{\Delta t}, \\ A_{\Delta t}, & \Delta Z > A_{\Delta t}, \\ -A_{\Delta t}, & \Delta Z < -A_{\Delta t}. \end{cases} \quad (2.48)$$

where $\Delta \tilde{Z}_{\Delta t}$ is bounded by $A_{\Delta t} := \sqrt{2k|\ln \Delta t|}, k \geq 1$.

These increments satisfy ($\mathbb{E}[\Delta \tilde{Z}_{\Delta t}] = \mathbb{E}[\Delta Z_{\Delta t}] = 0$) and the following inequalities

$$0 \leq \mathbb{E}[(\Delta Z - \Delta \tilde{Z})^2] \leq \Delta t^k, \quad \mathbb{E}[(\Delta Z)^2] - \mathbb{E}[(\Delta \tilde{Z})^2] \leq \left(1 + \frac{4}{\sqrt{\pi}}\sqrt{k|\ln \Delta t|}\right) \Delta t^k. \quad (2.49)$$

$$\mathbb{E}[(\Delta Z^2 - \Delta \tilde{Z}^2)(\Delta Z - \Delta \tilde{Z})] = 0, \quad (2.50)$$

The first two inequalities are established in [49] and are elaborated upon in Appendix A.3, and all three are required later in this paper.

When using increments sampled from the normal distribution, the Euler Maruyama scheme method 2.1, is not convergent to the Stratonovich system eq. (2.1), it converges to the Itô system (eq. (2.3)) with mean square order 1/2. When using increments sampled from the normal distribution, the SARK method (method 2.3) converges to the following SDE

$$d\mathbf{q} = (\lambda_0 \mathbf{f}(\mathbf{q}) + \lambda_1 DG|_{\mathbf{q}}G(\mathbf{q})) dt + \lambda_2 G(\mathbf{q})d\mathbf{W}, \quad \lambda_1 = \sum_{j=1}^s \tilde{b}_j \left(\sum_{k=1}^s \tilde{a}_{jk} \right), \quad \lambda_0 = \sum_{j=1}^s b_j, \quad \lambda_2 = \sum_{j=1}^s \tilde{b}_j. \quad (2.51)$$

This allows the SARK method 2.3 convergence to either Itô eq. (2.3) or Stratonovich eq. (2.1) upon appropriate Butcher tableau choices, and we shall refer to the SDE specified by the butcher tableau as the ‘‘Ruemelin-SDE’’. The order one deterministic ARK scheme conditions $b^T e = \tilde{b}^T e = 1 = \lambda_2 = \lambda_1$, are required to capture $\mathbf{f}, Gd\mathbf{W}$ terms. The condition $\tilde{b}^T \tilde{A}e = 1/2 = \lambda_1$, allows convergence to the Stratonovich equation by attaining the Itô-Stratonovich correction through numerical approximation, whereas the condition $\tilde{b}^T \tilde{A}e = 0 = \lambda_1$, allows convergence to the Itô equation.

Assumption 2.1 (MS convergence). Let \mathbf{q}^{n+1} , be the solution to the Stochastic Additive Runge-Kutta method 2.3 from the initial condition \mathbf{q}^n , let $\mathbf{q}(t^{n+1})$, be the solution to the Rumelin SDE eq. (2.51) from the initial condition \mathbf{q}^n , using the normal increments $\Delta \mathbf{W}$. We shall assume the following mean square local error estimates

$$\|\mathbb{E}[\mathbf{q}(t^{n+1}) - \mathbf{q}^{n+1}]\|_2 = \mathcal{O}(\Delta t^{p_1}), \quad (2.52)$$

$$(\mathbb{E}[\|\mathbf{q}(t^{n+1}) - \mathbf{q}^{n+1}\|_2^2])^{1/2} = \mathcal{O}(\Delta t^{p_2}), \quad (2.53)$$

$p_1 \geq p_2 + 1/2, p_2 \geq 1$, where we shall for convenience take $p_2 = 1$.

These local estimate need not be assumed but may be proven by Taylor expanding the numerical method and taking the difference from a Stratonovich Taylor (Wagner-Platen) expansion. These local error estimates are commonly assumed in light of the fundamental theorem of mean square convergence [49], required for the mean square order 1/2 of the numerical scheme described below.

Theorem 2.3 (G. N. Milstein, M. V. Tretyakov, Fundamental theorem on mean square convergence [50]). Suppose an approximation \mathbf{q}^{n+1} and the exact solution $\mathbf{q}(t^{n+1})$ both starting from the arbitrary initial condition $\mathbf{q}^n \in \mathbb{R}^d$ satisfy the following local error estimates,

$$\|\mathbb{E}[\mathbf{q}(t^{n+1}) - \mathbf{q}^{n+1}]\|_2 \leq L (1 + \|\mathbf{q}^n\|_2^2)^{1/2} \Delta t^{p_1}, \quad (2.54)$$

$$[\mathbb{E}[\|\mathbf{q}(t^{n+1}) - \mathbf{q}^{n+1}\|_2^2]]^{1/2} \leq L (1 + \|\mathbf{q}^n\|_2^2)^{1/2} \Delta t^{p_2}. \quad (2.55)$$

Where L denotes an arbitrary constant, not necessarily the same in each equation. If both

$$p_1 \geq p_2 + \frac{1}{2}, \quad p_2 \geq \frac{1}{2}.$$

Then for the entire time interval $n = 0, 1, \dots, N$ the following inequality holds:

$$[\mathbb{E}[\|\mathbf{q}(t^n) - \mathbf{q}^{n+1}\|_2^2]]^{1/2} \leq L (1 + \mathbb{E}[\|\mathbf{q}_0\|_2^2])^{1/2} \Delta t^{p_2 - 1/2}, \quad (2.56)$$

i.e. the global mean square order of accuracy of the method is $p = p_2 - 1/2$.

Remark. Since in this work we do not consider approximating higher-order stochastic integrals it is sufficient to show

$$p_1 \geq 3/2, \quad p_2 \geq 1. \quad (2.57)$$

to prove global mean square convergence order 1/2.

We wish to prove convergence of the SRK, SARK, and SGARK, schemes when using bounded increments in eq. (2.70) and wish to use theorem 2.3. To do so we use lemma 2.1 below introduced in [49] where if one adds and subtracts the unbounded increment system, one can require local error estimates between the bounded and unbounded increment-driven system sufficient to prove convergence of the bounded increment-driven system to the exact solution of the SDE.

Lemma 2.1 (Convergence [49]). Let $\mathbf{q}(t^{n+1})$, be the analytic solution to the Rumelin SDE eq. (2.51) from the initial condition \mathbf{q}^n . Let \mathbf{q}^{n+1} , be the solution to the Stochastic Additive Runge-Kutta method 2.3 from the initial condition \mathbf{q}^n , using a P -dimensional normally distributed variable $\Delta Z^P \sim N(0, 1)$. Let $\tilde{\mathbf{q}}^{n+1}$, be the solution to the Stochastic Additive Runge-Kutta method 2.3 from the initial condition \mathbf{q}^n , using the bounded increments $\Delta \tilde{Z}$ in eq. (2.48). Then the following conditions bounding the difference between the two numerical methods

$$\mathbb{E}[\mathbf{q}^{n+1} - \tilde{\mathbf{q}}^{n+1}] = \mathcal{O}(\Delta t^{p_1}) \quad (2.58)$$

$$(\mathbb{E}[\|\mathbf{q}^{n+1} - \tilde{\mathbf{q}}^{n+1}\|_2^2])^{1/2} = \mathcal{O}(\Delta t^{p_2}). \quad (2.59)$$

where $p_1 \geq p_2 + 1/2$, $p_2 \geq 1/2$, are sufficient (by theorem 2.3), to establish the bounded increment-driven system is also convergent with mean square order $p_2 - 1/2$.

Proof. Established in [49] it is sufficient by the fundamental theorem on mean square convergence that the following identities are satisfied,

$$\mathbb{E}[\mathbf{q}(t^{n+1}) - \tilde{\mathbf{q}}^{n+1}] = \mathbb{E}[\mathbf{q}(t^{n+1}) - \mathbf{q}^{n+1} + \mathbf{q}^{n+1} - \tilde{\mathbf{q}}^{n+1}] = \mathcal{O}(\Delta t^{p_1}), \quad (2.60)$$

$$(\mathbb{E}[\|\mathbf{q}(t^{n+1}) - \tilde{\mathbf{q}}^{n+1}\|_2^2])^{1/2} = (\mathbb{E}[\|\mathbf{q}(t^{n+1}) - \mathbf{q}^{n+1} + \mathbf{q}^{n+1} - \tilde{\mathbf{q}}^{n+1}\|_2^2])^{1/2} = \mathcal{O}(\Delta t^{p_2}), \quad (2.61)$$

for $p_1 \geq p_2 + 1/2$, $p_2 \geq 1/2$, for order $p_2 - 1/2$ convergence. It has been assumed that the numerical method for unbounded increments already satisfies eqs. (2.52) and (2.53). Therefore the following equalities

$$\mathbb{E}[\mathbf{q}^{n+1} - \tilde{\mathbf{q}}^{n+1}] = \mathcal{O}(\Delta t^{p_1}), \quad (2.62)$$

$$(\mathbb{E}[\|\mathbf{q}^{n+1} - \tilde{\mathbf{q}}^{n+1}\|_2^2] + 2\mathbb{E}[(\mathbf{q}^{n+1} - \tilde{\mathbf{q}}^{n+1})^T(\mathbf{q}(t^{n+1}) - \mathbf{q}^{n+1})])^{1/2} = \mathcal{O}(\Delta t^{p_2}), \quad (2.63)$$

are sufficient for order $p_2 - 1/2$. This further simplifies noting $\mathbb{E}[\mathbf{a}^T \mathbf{b}] \leq \mathbb{E}[\|\mathbf{a}^T \mathbf{b}\|] \leq \mathbb{E}[\|\mathbf{a}\|_2^2]^{1/2} \mathbb{E}[\|\mathbf{b}\|_2^2]^{1/2}$, to

$$\mathbb{E}[\mathbf{q}^{n+1} - \tilde{\mathbf{q}}^{n+1}] = \mathcal{O}(\Delta t^{p_1}), \quad (2.64)$$

$$(\mathbb{E}[\|\mathbf{q}^{n+1} - \tilde{\mathbf{q}}^{n+1}\|_2^2])^{1/2} = \mathcal{O}(\Delta t^{p_2}). \quad (2.65)$$

□

Using lemma 2.1 we show the EM scheme converges to the Itô system eq. (2.3) when using bounded increments $\Delta \tilde{\mathbf{Z}}$ in eq. (2.48) rather than $\Delta \mathbf{Z}$ normal ones.

Example 2.3 ([50]). Let $\mathbf{q}^{(1)} := \mathbf{q} + \Delta t f(\mathbf{q}) + t^{1/2} G(\mathbf{q}) \Delta \mathbf{Z}$, be a solution of one step EM scheme, converging with strong order 1/2 to the Itô system eq. (2.3). Let $\mathbf{q}^{(2)} := \mathbf{q} + \Delta t f(\mathbf{q}) + t^{1/2} G(\mathbf{q}) \Delta \tilde{\mathbf{Z}}$, be a solution of the one step bounded increment driven system eq. (2.48). Then the difference between the two solutions from the same initial condition \mathbf{q} satisfies

$$\mathbf{q}^{(1)} - \mathbf{q}^{(2)} = t^{1/2} G(\mathbf{q}) [\Delta \mathbf{Z} - \Delta \tilde{\mathbf{Z}}], \quad (2.66)$$

after one time step. Through the centered properties of the increments $(\mathbf{Z}, \tilde{\mathbf{Z}})$ we have the first local error estimate $\|\mathbb{E}[\mathbf{q}^1 - \mathbf{q}^2]\|_2 = 0$, and by the properties of matrix norms and eq. (2.49) one has,

$$\mathbb{E}[\|\mathbf{q}^1 - \mathbf{q}^2\|_2^2] \leq t \|G(\mathbf{q})\|_2^2 \mathbb{E}[\|\Delta \mathbf{Z} - \Delta \tilde{\mathbf{Z}}\|_2^2] = t \|G(\mathbf{q})\|_2^2 \sum_{p=1}^P \mathbb{E}[(\Delta Z^p - \Delta \tilde{Z}^p)^2] \leq P \|G\|_2^2 \Delta t^{k+1}. \quad (2.67)$$

Then by the growth bound assumption required for well-posedness of the SDE in section 2.2, one has

$$(\mathbb{E}[\|\mathbf{q}^1 - \mathbf{q}^2\|_2^2])^{1/2} \leq \sqrt{PL} (1 + \|\mathbf{q}\|_2^2)^{1/2} \Delta t^{(k+1)/2} \quad (2.68)$$

These local error estimates are sufficient when $k \geq 1$, by the FTMSC theorem 2.3 and lemma 2.1 with $p_1 = \infty$, and $p_2 = (k + 1)/2$ for mean square convergence order 1/2 of the bounded increment driven system.

Using lemma 2.1 and appendices Appendix A.2 and Appendix A.3, we similarly establish method 2.3 when driven by bounded increments as in definition 2.5 one attains the same mean square convergence to the Rumelin-SDE as when using normally distributed increments. A similar statement is made in [49, 50] however, a detailed proof involving regularity conditions is not provided.

Theorem 2.4 (MS Convergence of bounded increment SARK method 2.3.). The difference between the one step bounded increment $(\Delta \tilde{\mathbf{Z}})$ system $\tilde{\mathbf{q}}^{n+1}$, and the one step normally distributed driven $(\Delta \mathbf{Z})$ system \mathbf{q}^{n+1} , both starting from the same initial condition $\mathbf{q} = \mathbf{q}^n$ and using the same ARK method 2.3, satisfy the following local error estimates

$$\mathbb{E}[\mathbf{q}^{n+1} - \tilde{\mathbf{q}}^{n+1}] = \mathcal{O}(\Delta t^{\min\{3/2, k+1-\epsilon\}}), \quad (\mathbb{E}[\|\mathbf{q}^{n+1} - \tilde{\mathbf{q}}^{n+1}\|_2^2])^{1/2} = \mathcal{O}(\Delta t^{\min\{1, (k+1)/2\}}), \quad (2.69)$$

where ϵ is a small positive number. Provided that the Butcher tableau's $((A, b), (\tilde{A}, \tilde{b})) = ((a_{i,j}, b_j), (\tilde{a}_{i,j}, \tilde{b}_j))$ are componentwise bounded, the drift and diffusion are componentwise twice continuously differentiable $f^k \in C^2(\mathbb{R}^d; \mathbb{R})$, $g_p^k \in C^2(\mathbb{R}^d; \mathbb{R})$, $\forall p \in \{1, \dots, P\}$, $\forall k \in \{1, \dots, d\}$, and $DG|_{\mathbf{q}}$, $G(\mathbf{q})$, $Df|_{\mathbf{q}}$, $f(\mathbf{q})$ are bounded. The above local error estimates in combination with theorem 2.3 and lemma 2.1 are sufficient, to prove mean square convergence order 1/2 of the SARK method 2.3 (to the Rumelin-SDE) when using the bounded increments in definition 2.5 with $k \geq 1$.

Proof. theorem 2.4. The difference between, the SSPARK method 2.3, with bounded increments $\Delta\tilde{\mathbf{Z}}$ eq. (2.48) and without bounded increments using normally distributed random variable $\Delta\mathbf{Z}$, both starting from the initial condition \mathbf{q} , is

$$\mathbf{q}^{n+1} - \tilde{\mathbf{q}}^{n+1} = \Delta t \sum_{i=1}^s b_i [\mathbf{f}(\mathbf{k}^i) - \mathbf{f}(\tilde{\mathbf{k}}^i)] + \sqrt{\Delta t} \sum_{i=1}^s \tilde{b}_i \left[G(\mathbf{k}^i) \Delta\mathbf{Z} - G(\tilde{\mathbf{k}}^i) \Delta\tilde{\mathbf{Z}} \right], \quad (2.70)$$

where the substages are

$$\mathbf{k}^i = \mathbf{q}^n + \Delta t \sum_{j=1}^s a_{i,j} \mathbf{f}(\mathbf{k}^j) + (\Delta t)^{1/2} \sum_{j=1}^s \tilde{a}_{i,j} G(\mathbf{k}^j) \Delta\mathbf{Z}, \quad (2.71)$$

$$\tilde{\mathbf{k}}^i = \mathbf{q}^n + \Delta t \sum_{j=1}^s a_{i,j} \mathbf{f}(\tilde{\mathbf{k}}^j) + (\Delta t)^{1/2} \sum_{j=1}^s \tilde{a}_{i,j} G(\tilde{\mathbf{k}}^j) \Delta\tilde{\mathbf{Z}}. \quad (2.72)$$

Now Taylor expand G , about \mathbf{q}^n . Note that $G : \mathbb{R}^d \rightarrow \mathbb{R}^{d \times P}$, is defined with columns $\mathbf{g}_p : \mathbb{R}^d \rightarrow \mathbb{R}^d$, such that the derivative of G with respect to \mathbf{q} evaluated at \mathbf{a} , is denoted $DG|_{\mathbf{a}}$ and can be thought of as a linear map taking values to $\mathbb{R}^{d \times P \times d}$. We require that the k -th component of \mathbf{g}_p is continuous, and twice continuously differentiable within an open ball centered at \mathbf{q} containing $\mathbf{q} + \mathbf{a}$, to apply a component-wise multivariate Taylor theorem.

$$G(\mathbf{k}^i) = G(\mathbf{q}) + DG|_{\mathbf{q}} \underbrace{\left(\Delta t \sum_{j=1}^s a_{i,j} \mathbf{f}(\mathbf{k}^j) + (\Delta t)^{1/2} \sum_{j=1}^s \tilde{a}_{i,j} G(\mathbf{k}^j) \Delta\mathbf{Z} \right)}_{:=\mathbf{a}} + R_1(\mathbf{q}, \mathbf{a}), \quad (2.73)$$

$$G(\tilde{\mathbf{k}}^i) = G(\mathbf{q}) + DG|_{\mathbf{q}} \underbrace{\left(\Delta t \sum_{j=1}^s a_{i,j} \mathbf{f}(\tilde{\mathbf{k}}^j) + (\Delta t)^{1/2} \sum_{j=1}^s \tilde{a}_{i,j} G(\tilde{\mathbf{k}}^j) \Delta\tilde{\mathbf{Z}} \right)}_{:=\tilde{\mathbf{a}}} + R_2(\mathbf{q}, \tilde{\mathbf{a}}). \quad (2.74)$$

Where $R_1(\mathbf{q}, \mathbf{a})$, $R_2(\mathbf{q}, \tilde{\mathbf{a}})$, are remainder terms satisfying the following bounds $\|R_1(\mathbf{q}, \mathbf{a})\|_2 \leq L\|\mathbf{a}\|^2$, $\|R_2(\mathbf{q}, \tilde{\mathbf{a}})\|_2 \leq L\|\tilde{\mathbf{a}}\|^2$. We similarly require that the k -th component of \mathbf{f} is continuous and twice continuously differentiable within an open ball centered at \mathbf{q} containing $\mathbf{q} + \mathbf{a}$, to apply a component-wise multivariate Taylor theorem as follows

$$\mathbf{f}(\mathbf{k}^i) = \mathbf{f}(\mathbf{q}) + D\mathbf{f}|_{\mathbf{q}} \mathbf{a} + \mathbf{R}_3(\mathbf{q}, \mathbf{a}), \quad (2.75)$$

$$\mathbf{f}(\tilde{\mathbf{k}}^i) = \mathbf{f}(\mathbf{q}) + D\mathbf{f}|_{\mathbf{q}} \tilde{\mathbf{a}} + \mathbf{R}_4(\mathbf{q}, \tilde{\mathbf{a}}). \quad (2.76)$$

Where $\|\mathbf{R}_3(\mathbf{q}, \mathbf{a})\|_2 \leq L\|\mathbf{a}\|_2^2$, $\|\mathbf{R}_4(\mathbf{q}, \tilde{\mathbf{a}})\|_2 \leq L\|\tilde{\mathbf{a}}\|_2^2$. So that the difference can be written as

$$\mathbf{q}^{n+1} - \tilde{\mathbf{q}}^{n+1} = \Delta t \sum_{i=1}^s b_i [DF|_{\mathbf{q}}(\mathbf{a} - \tilde{\mathbf{a}})] + \Delta t \sum_{i=1}^s b_i [R_3(\mathbf{q}, \mathbf{a}) - R_4(\mathbf{q}, \tilde{\mathbf{a}})] + \sqrt{\Delta t} \sum_{i=1}^s \tilde{b}_i G(\mathbf{q}) [\Delta\mathbf{Z} - \Delta\tilde{\mathbf{Z}}] \quad (2.77)$$

$$+ \sqrt{\Delta t} \sum_{i=1}^s \tilde{b}_i DG|_{\mathbf{q}}(\mathbf{a} \Delta\mathbf{Z} - \tilde{\mathbf{a}} \Delta\tilde{\mathbf{Z}}) + \sqrt{\Delta t} \sum_{i=1}^s \tilde{b}_i \left(R_1(\mathbf{q}, \mathbf{a}) \Delta\mathbf{Z} - R_2(\mathbf{q}, \tilde{\mathbf{a}}) \Delta\tilde{\mathbf{Z}} \right). \quad (2.78)$$

Now Taylor expanding terms in $\mathbf{a}, \tilde{\mathbf{a}}$, about \mathbf{q} gives the following

$$\Delta t \sum_{i=1}^s b_i [DF|_{\mathbf{q}}(\mathbf{a} - \tilde{\mathbf{a}})] = \Delta t \sum_{i=1}^s b_i DF|_{\mathbf{q}} \left((\Delta t)^{1/2} \sum_{j=1}^s \tilde{a}_{i,j} G(\mathbf{q}) [\Delta\mathbf{Z} - \Delta\tilde{\mathbf{Z}}] + \mathcal{O}(\Delta t) \right), \quad (2.79)$$

$$\Delta t^{1/2} \sum_{i=1}^s \tilde{b}_i DG|_{\mathbf{q}}(\mathbf{a} \Delta\mathbf{Z} - \tilde{\mathbf{a}} \Delta\tilde{\mathbf{Z}}) = \Delta t^{1/2} \sum_{i=1}^s \tilde{b}_i DG|_{\mathbf{q}} \left[\Delta t^{1/2} \sum_{j=1}^s \tilde{a}_{i,j} G(\mathbf{q}) (\Delta\mathbf{Z} - \Delta\tilde{\mathbf{Z}}) + \mathcal{O}(\Delta t) \right]. \quad (2.80)$$

Substituting these expressions (into eq. (2.78)), gives the following expression

$$\mathbf{q}^{n+1} - \tilde{\mathbf{q}}^{n+1} = \sqrt{\Delta t} \sum_{i=1}^s \tilde{b}_i G(\mathbf{q}^n) [\Delta \mathbf{Z} - \Delta \tilde{\mathbf{Z}}] + (\Delta t)^{3/2} \sum_{i=1}^s DF|_{\mathbf{q}} \sum_{j=1}^s \tilde{a}_{i,j} \left[G(\mathbf{k}^j) \Delta \mathbf{Z} - G(\tilde{\mathbf{k}}^j) \Delta \tilde{\mathbf{Z}} \right] \quad (2.81)$$

$$+ \Delta t \sum_{i=1}^s \tilde{b}_i DG|_{\mathbf{q}} \sum_{j=1}^s \tilde{a}_{i,j} \left[G(\mathbf{k}^j) \Delta \mathbf{Z} \otimes \Delta \mathbf{Z} - G(\tilde{\mathbf{k}}^j) \Delta \tilde{\mathbf{Z}} \otimes \Delta \tilde{\mathbf{Z}} \right] + \mathcal{O}(\Delta t^{3/2}) \quad (2.82)$$

Where for notational convenience we have written $DG_{\mathbf{q}}(G_{\mathbf{q}} \Delta \mathbf{Z}) \Delta \mathbf{Z} = DG_{\mathbf{q}} G_{\mathbf{q}} (\Delta \mathbf{Z} \otimes \Delta \mathbf{Z})$, and have used the remainder bounds from Taylor's theorem [Appendix A.2](#) and [Appendix A.3](#) to establish the other terms are higher order terms. The subsequent Taylor expansion of G again leads to (at leading order) the following expression

$$\mathbf{q}^{n+1} - \tilde{\mathbf{q}}^{n+1} = \sqrt{\Delta t} G(\mathbf{q}) \sum_{i=1}^s \tilde{b}_i [\Delta \mathbf{Z} - \Delta \tilde{\mathbf{Z}}] + \Delta t DG|_{\mathbf{q}} G(\mathbf{q}) \sum_{i=1}^s \tilde{b}_i \sum_{j=1}^s \tilde{a}_{i,j} \left[\Delta \mathbf{Z} \otimes \Delta \mathbf{Z} - \Delta \tilde{\mathbf{Z}} \otimes \Delta \tilde{\mathbf{Z}} \right] \quad (2.83)$$

$$+ (\Delta t)^{3/2} DF|_{\mathbf{q}} G(\mathbf{q}) \sum_{i=1}^s \sum_{j=1}^s \tilde{a}_{i,j} \left[\Delta \mathbf{Z} - \Delta \tilde{\mathbf{Z}} \right] + \mathcal{O}(\Delta t^{3/2}). \quad (2.84)$$

Now since $(a_{i,j}, b_j)$, $(\tilde{a}_{i,j}, \tilde{b}_j)$ are assumed finite, taking the expectation sets the first term to zero by the symmetric property of $\Delta \mathbf{Z}$ and $\Delta \tilde{\mathbf{Z}}$. The i, j -th component of $(\Delta \mathbf{Z} \otimes \Delta \mathbf{Z})_{i,j}$, also vanishes for $i \neq j$ in expectation, leaving at leading order an error associated with numerically approximating the Itô-Stratonovich correction by using bounded increments (as opposed to normally distributed ones). This can be bounded as follows

$$\mathbb{E}[\mathbf{q}^{n+1} - \tilde{\mathbf{q}}^{n+1}] = \Delta t \sum_{i=1}^s \tilde{b}_i \sum_{i=1}^s \tilde{a}_{i,j} DG|_{\mathbf{q}} G(\mathbf{q}) P(1 - \mathbb{E}[\Delta \tilde{\mathbf{Z}}^p]) + \mathcal{O}(\Delta t^{3/2}) \quad (2.85)$$

$$\leq (\tilde{\mathbf{b}}^T \tilde{A} \mathbf{e}) DG|_{\mathbf{q}} G(\mathbf{q}) P \left(1 + \frac{4}{\sqrt{\pi}} \sqrt{k |\ln(\Delta t)|} \right) \Delta t^{k+1} + \mathcal{O}(\Delta t^{3/2}). \quad (2.86)$$

Sufficient to conclude that the leading order term is $\mathcal{O}(\Delta t^{\min\{k+1-\epsilon, 3/2\}})$ where $\epsilon > 0$ is a small number. Then consider the square of the difference,

$$\mathbb{E}[\|\mathbf{q}^{n+1} - \tilde{\mathbf{q}}^{n+1}\|_2^2] \leq \Delta t \|G(\mathbf{q})\|_2^2 \left(\sum_{i=1}^s b_i \right)^2 \mathbb{E}[\|\Delta \mathbf{Z} - \Delta \tilde{\mathbf{Z}}\|_2^2] \quad (2.87)$$

$$+ \mathbb{E} \left[\underbrace{\Delta t^{3/2} (\tilde{\mathbf{b}}^T \mathbf{e}) (\tilde{\mathbf{b}}^T \tilde{A} \mathbf{e}) \frac{\partial g_p^k}{\partial q^j} g_q^j g_r^k \left(\Delta Z^p \Delta Z^q - \Delta \tilde{Z}^p \Delta \tilde{Z}^q \right) (\Delta Z^r - \Delta \tilde{Z}^r)}_{\text{underbraced term}} + \mathcal{O}(\Delta t^2) \right]. \quad (2.88)$$

It needs to be shown that the underbraced term (where summation notation is adopted for convenience) is order higher order than 2. This underbraced term vanishes due to Isserlis theorem and symmetry of the distribution and using the inequality established when considering the total law of expectation conditioned on the events $(Z < -A, |Z| < A, Z > A)$ when $p = q = r$. So that we attain the following estimate

$$\mathbb{E}[\|\mathbf{q}^{n+1} - \tilde{\mathbf{q}}^{n+1}\|_2^2]^{1/2} \leq \mathcal{O} \left(\Delta t^{\min\{1, (1+k)/2\}} \right) \quad (2.89)$$

Then by the FTMSC theorem [2.3](#) and lemma [2.1](#), eqs. (2.86) and (2.89) imply mean square order $p_2 - 1/2$ convergence when the conditions $p_2 = \min\{(k+1)/2, 1\} \geq 1$, $p_1 = \min\{k+1-\epsilon, 3/2\} \geq 3/2$ are met, $k \geq 1$, is sufficient in the limit of small Δt for MS convergence order $1/2$. \square

We would also like to remark that this can extend to the generalised setting of SGARK schemes including method [2.4](#) in a similar manner in lemma [2.2](#) below.

Lemma 2.2 (GARK extension). Let $\tilde{\mathbf{q}}^{n+1}$ be the solution driven by bounded increments definition 2.5 with $k \geq 1$, and the normally distributed driven system \mathbf{q}^{n+1} , for any GARK scheme, then for $f^k \in C^2(\mathbb{R}^d; \mathbb{R})$, $g_p^k \in C^2(\mathbb{R}^d; \mathbb{R})$, $\forall p \in \{1, \dots, P\}$, $\forall k \in \{1, \dots, d\}$. One has the following mean square estimates,

$$\mathbb{E}[\mathbf{q}^{n+1} - \tilde{\mathbf{q}}^{n+1}] = \mathcal{O}(\Delta t^{\min\{k+1-\epsilon, 3/2\}}), \quad (\mathbb{E}[\|\mathbf{q}^{n+1} - \tilde{\mathbf{q}}^{n+1}\|_2^2])^{1/2} = \mathcal{O}(t^{\min\{(k+1)/2, 1\}}), \quad (2.90)$$

given $DG|_{\mathbf{q}}, G(\mathbf{q}), DF|_{\mathbf{q}}, F(\mathbf{q})$ are bounded, and all components of all the Butcher-tableau's are component-wise bounded.

Proof. Consider the difference

$$\mathbf{q}^{n+1} - \tilde{\mathbf{q}}^{n+1} = \Delta t \sum_{i=1}^{s^f} b_i^f \left(\mathbf{f}(\mathbf{k}_i^f) - \mathbf{f}(\tilde{\mathbf{k}}_i^f) \right) + \sqrt{\Delta t} \sum_{i=1}^{s^g} b_i^g \left(G(\mathbf{k}_i^g) \Delta \mathbf{Z} - G(\tilde{\mathbf{k}}_i^g) \Delta \tilde{\mathbf{Z}} \right), \quad (2.91)$$

and then consider Taylor expansions around \mathbf{q} where

$$\mathbf{k}_i^f = \mathbf{q} + \Delta t \sum_{j=1}^{s^f} a_{i,j}^{f,f} \mathbf{f}(\mathbf{k}_j^f) + \sqrt{\Delta t} \sum_{j=1}^{s^g} a_{i,j}^{f,g} G(\mathbf{k}_j^g) \Delta \mathbf{Z}, \quad \tilde{\mathbf{k}}_i^f = \mathbf{q} + \Delta t \sum_{j=1}^{s^f} a_{i,j}^{f,f} \mathbf{f}(\tilde{\mathbf{k}}_j^f) + \sqrt{\Delta t} \sum_{j=1}^{s^g} a_{i,j}^{f,g} G(\tilde{\mathbf{k}}_j^g) \Delta \tilde{\mathbf{Z}}, \quad (2.92)$$

$$\mathbf{k}_i^g = \mathbf{q} + \Delta t \sum_{j=1}^{s^f} a_{i,j}^{g,f} \mathbf{f}(\mathbf{k}_j^f) + \sqrt{\Delta t} \sum_{j=1}^{s^g} a_{i,j}^{g,g} G(\mathbf{k}_j^g) \Delta \mathbf{Z}, \quad \tilde{\mathbf{k}}_i^g = \mathbf{q} + \Delta t \sum_{j=1}^{s^f} a_{i,j}^{g,f} \mathbf{f}(\tilde{\mathbf{k}}_j^f) + \sqrt{\Delta t} \sum_{j=1}^{s^g} a_{i,j}^{g,g} G(\tilde{\mathbf{k}}_j^g) \Delta \tilde{\mathbf{Z}}, \quad (2.93)$$

so that

$$\mathbf{q}^{n+1} - \tilde{\mathbf{q}}^{n+1} = \sqrt{\Delta t} \sum_{i=1}^{s^g} \tilde{b}_i^g G(\mathbf{q}) (\Delta \mathbf{Z} - \Delta \tilde{\mathbf{Z}}) \quad (2.94)$$

$$+ \Delta t \sum_{i=1}^{s^g} \tilde{b}_i^g \left(\sum_{j=1}^{s^g} \tilde{a}_{i,j}^{g,g} DG|_{\mathbf{q}}(G(\mathbf{q}) \Delta \mathbf{Z}) \Delta \mathbf{Z} - \sum_{j=1}^{s^g} \tilde{a}_{i,j}^{g,g} DG|_{\mathbf{q}}(G(\mathbf{q}) \Delta \tilde{\mathbf{Z}}) \Delta \tilde{\mathbf{Z}} \right) + \mathcal{O}(\Delta t^{3/2}), \quad (2.95)$$

as before in expectation one can show, that the leading order terms are

$$\mathbb{E}[\mathbf{q}^{n+1} - \tilde{\mathbf{q}}^{n+1}] \leq (\tilde{b}^g \tilde{A}^{g,g} e + \tilde{b}^g \tilde{A}^{f,g} e) DG|_{\mathbf{q}} G(\mathbf{q}) P \left(1 + \frac{4}{\sqrt{\pi}} \sqrt{k |\ln(\Delta t)|} \right) \Delta t^{k+1} + \mathcal{O}(\Delta t^{3/2}) \quad (2.96)$$

$$\leq \mathcal{O}(\Delta t^{\min\{k+1-\epsilon, 3/2\}}), \quad (2.97)$$

$$\mathbb{E}[\|\mathbf{q}^{n+1} - \tilde{\mathbf{q}}^{n+1}\|_2^2] \leq \Delta t \|G(\mathbf{q})\|_2^2 \left(\sum_{i=1}^{s^g} \tilde{b}_i^g \right)^2 \mathbb{E}[\|\Delta \mathbf{Z} - \Delta \tilde{\mathbf{Z}}\|_2^2] + \mathcal{O}(\Delta t^2) \leq \mathcal{O}(t^{\min\{k+1, 2\}}). \quad (2.98)$$

These are sufficient for the bounded increment-driven system to converge to the same solution as the unbounded increment-driven system, with the same mean square order of 1/2. \square

3. Practical Methods and Numerical Demonstrations

3.1. Practical Methods

We state some common strong stability preserving numerical integrators in their canonical Shu-Osher form when we replace the forward Euler method with the Euler Maruyama scheme. The Shu-Osher representation of the numerical schemes is typically computationally efficient in terms of memory allocation and allows easy implementation.

SSP Stochastic Runge-Kutta

Method 3.1 (SSP22 Stratonovich (Heun)). The two-stage second-order strong stability preserving Stochastic Runge-Kutta method

$$\mathbf{q}^1 = \text{EM}(\mathbf{q}^n) \quad (3.1)$$

$$\mathbf{q}^{n+1} = \frac{1}{2}\mathbf{q}^n + \frac{1}{2}\text{EM}(\mathbf{q}^1). \quad (3.2)$$

converges to the Stratonovich form of the equation eq. (2.1), with weak order 1 using the increments in eq. (2.45), and mean square (strong order) 1/2 using the increments definition 2.5. The scheme is SSP in the stochastic setting with a radius of monotonicity 1.

Method 3.2 (SSP33 Stratonovich (Shu-Osher method)).

$$\mathbf{q}^1 = \text{EM}(\mathbf{q}^n) \quad (3.3)$$

$$\mathbf{q}^1 = \frac{3}{4}\mathbf{q}^n + \frac{1}{4}\text{EM}(\mathbf{q}^1) \quad (3.4)$$

$$\mathbf{q}^{n+1} = \frac{1}{3}\mathbf{q}^n + \frac{2}{3}\text{EM}(\mathbf{q}^1) \quad (3.5)$$

converges to the Stratonovich form of the equation eq. (2.1), with weak order 1 when using the bounded increments in eq. (2.45), and (mean square) strong order 1/2 when using bounded increments in eq. (2.48). And is contractive/SSP when the Euler Maruyama scheme is, with radius of monotonicity 1.

Method 3.3 (SSP104-Stratonovich-(Ketcherson [34])). Let the time Scaled Euler Maruyama be denoted by

$$\mathbf{q}^{n+1} = \text{EM}(a\Delta t, \mathbf{q}) = \mathbf{q}^n + a\mathbf{f}(\mathbf{q}^n)\Delta t + a^{1/2}\sum_p \mathbf{g}_p(\mathbf{q}^n)\Delta \mathbf{S}^p, \quad (3.6)$$

then the SSP104-Stratonovich-(Ketcherson) method can be defined as follows

$$\mathbf{q}^0 = \mathbf{q}^n, \quad (3.7)$$

$$\mathbf{q}^{i+1} = \text{EM}(1/6, \mathbf{q}^i), \quad \text{for } i = 0, 1, 2, 3, \quad (3.8)$$

$$\mathbf{q}^5 = \frac{3}{5}\mathbf{q}^0 + \frac{2}{5}\text{EM}(1/6, \mathbf{q}^4), \quad (3.9)$$

$$\mathbf{q}^{i+1} = \text{EM}(1/6, \mathbf{q}^i), \quad \text{for } i = 5, 6, 7, 8, \quad (3.10)$$

$$\mathbf{q}^{n+1} = \frac{1}{25}\mathbf{q}^n + \frac{9}{25}\text{EM}(1/6, \mathbf{q}^4) + \frac{15}{25}\text{EM}(1/6, \mathbf{q}^9). \quad (3.11)$$

converges to the Stratonovich form of the equation eq. (2.1), with weak order 1 using the increments in eq. (2.45), and mean square (strong order) 1/2 using the increments in definition 2.5. And is contractive with respect to arbitrary seminorms, when Euler Maruyama is, with radius of monotonicity 6.

SSP Stochastic Generalised Additive Runge-Kutta

Method 3.4 (SSP- Sequential Operator Splitting). We consider the following Sequential operator splitting method associated with Strang

$$\mathbf{q}^a = \text{SSP2m2}(\mathbf{q}^n, \mathbf{f}, \Delta t/2), \quad (3.12)$$

$$\mathbf{q}^b = \text{SSP2n2}(\mathbf{q}^a, G, \Delta \mathbf{S}), \quad (3.13)$$

$$\mathbf{q}^{n+1} = \text{SSP2m2}(\mathbf{q}^b, \mathbf{f}, \Delta t/2). \quad (3.14)$$

SSP2m2 is a $2m$ -stage RK method with radius of monotonicity $C = m$, equivalent to m stages of the SSP22 scheme above. Here the omission of G , $\Delta \mathbf{S}$ notationally implies this is a drift-only scheme, and the omission of $\mathbf{f}, \Delta t$ refers to this being a diffusion only scheme. The total method is SSP with time-step restriction $\min(2m\tau_f, n\tau_g)$. This scheme converges with weak order 1 when using the bounded increments eq. (2.45), and mean square (strong) order 0.5 when using increments in definition 2.5.

Method 3.5 (SSP-Additive Operator splitting). We consider the following additive operator splitting method (also attributable to Strang)

$$\mathbf{q}^a = \text{SSP2m2}(\mathbf{q}^n, \mathbf{f}, \Delta t), \quad \mathbf{q}^b = \text{SSP2n2}(\mathbf{q}^n, G, \Delta \mathbf{S}), \quad (3.15)$$

$$\mathbf{q}^{ba} = \text{SSP2n2}(\mathbf{q}^a, G, \Delta \mathbf{S}), \quad \mathbf{q}^{ab} = \text{SSP2m2}(\mathbf{q}^b, \mathbf{f}, \Delta t), \quad (3.16)$$

$$\mathbf{q}^{n+1} = 1/2(\mathbf{q}^{ab} + \mathbf{q}^{ba}). \quad (3.17)$$

Since this is also a convex combination this method has an SSP timestep criterion given by $\min(m\tau_f, n\tau_g)$. Therefore one can adjust m, n to attain a scheme of larger monotonicity and larger timestep based on \mathbf{f}, G . This scheme converges with weak order 1 to the Stratonovich system when using the bounded increments eq. (2.45), and mean square (strong) order 1/2 to the Stratonovich system when using increments eq. (2.48).

3.2. Numerical Demonstrations

3.2.1. Example 1a: Stochastic 2D Burgers equation, with slope limiters.

Theoretically, we have the following three sufficient properties required for a monotone solution,

1. A numerical method with a provable monotonic property for the Euler Maruyama map.
2. Bounded increments.
3. SSP time integration, with a non-zero radius of monotonicity.

We wish to numerically test what happens when these conditions are individually violated. To construct a numerical method with a provable monotonic property for the Euler Maruyama map, we use an approximate stochastic Riemann solver and the slope limiter framework in [59]. To construct a range-bounded solution with a type of local maximum principle. We consider the following 2D extension of the inviscid Burgers equation,

$$dq_t + \left(\left(\frac{1}{2}q^2 \right)_x + \left(\frac{1}{2}q^2 \right)_y \right) dt + (a(q)_x + b(q)_y) \circ dW_t = 0, \quad (3.18)$$

stochastically translated by a single uniform vector field (a, b) integrated in the Stratonovich sense against a one-dimensional Wiener process. This transforms the 2D-Burgers equation into a stochastic frame of reference, and the solution properties are unchanged from the 2D deterministic case. We shall first describe a numerical method with a specific provable monotonic property for the Euler Maruyama map. The following second-order finite volume method, with slope limiters, is described in [59] and summarised below.

Method 3.6 (FV2 with $N^2(K) \cup N(K)$ limiter [59]).

1. Project cell mean values to pointwise cell centered values $u_{i,j} = \mathcal{P}_2 \bar{u}_{i,j} = \bar{u}_{i,j}$, this direct evaluation is second order $\mathcal{O}(\Delta x^2 + \Delta y^2)$.
2. Get gradients within each cell $\{q_x, q_y\}$ using the pointwise cell centered values, the second order finite difference stencil $w_i = 1/2([1, 0, -1])^T$.
3. Create a linear subcell reconstruction within each cell $p_{i,j}(x) = \bar{u}_{i,j} + (x - x_i)u_x + (y - y_i)u_y$ from cell mean values and pointwise reconstructed gradients.
4. Reconstruct flux contributing edge defined values $u_{i,j}^R, u_{i,j}^L, u_{i,j}^U, u_{i,j}^D$ by evaluating the reconstructed polynomial. For example, the evaluation of $p_{i,j}$ at the right edge of cell (i, j) , at $(x_{i+1/2}, y_j)$, gives $u_{i,j}^R = u_{i,j} + 1/4(u_{i+1,j} - u_{i-1,j})$.
5. $N^2 \cup N(K)$ -MP Limiting procedure is employed to ensure an edge-defined local maximum principle specified in [59].
6. \mathcal{R} Resolve Riemann problem. Consider the Riemann problem at $(x_{i+1/2}, y_j)$. Where to the left of the edge discontinuity $q_{i+1/2}^L = q_i^R$, and to the right edge of the discontinuity we have $q_{i+1/2}^R = q_{i+1}^L$. This creates a discontinuous initial value problem known as a Riemann problem. This is resolvable exactly in the case of Burger's equation (Godunov's approach), or a stochastic extension of a Local Lax Friedrich flux definition 3.1.
7. \mathcal{F} Flux computation, quadrature, this is done through the midpoint rule (second order Gauss quadrature).

8. \mathcal{E} Evolve, the cell mean value by the fluxes, in a flux form forward Euler or Euler-Maruyama stage.

Whilst it may be possible to solve the exact Reimann problem for this particular problem, approximate Reimann solvers are cheaper and widely adopted for more complicated systems.

Definition 3.1 (LLF-EM-Stochastic Burgers equation Flux). Define the stochastic Euler Maruyama flux functions, as follows, using ideas from Kurganov and Tadmor [43],

$$\mathbb{F}(q, a) = \frac{1}{2}q^2 + aq \frac{\Delta W_t}{\Delta t}, \quad (3.19)$$

Compute the stochastic Euler-Maruyama maximum wave speed

$$\alpha_{i+1/2} = \max_{q \in \{q_{i+1/2}^L, q_{i+1/2}^R\}} \left| \frac{d}{dq} \mathbb{F}(q, a) \right| = \max \left\{ \left| a \Delta W / \Delta t + q_{i+1/2}^L \right|, \left| a \Delta W / \Delta t + q_{i+1/2}^R \right| \right\}. \quad (3.20)$$

and use these to define the stochastic Euler-Maruyama Local Lax Friedrich (Rusanov) flux

$$f_{i+1/2} = \frac{1}{2} \left(\mathbb{F}(q_{i+1/2}^L, a) + \mathbb{F}(q_{i+1/2}^R, a) \right) - \frac{1}{2} \alpha_{i+1/2} (q_{i+1/2}^R - q_{i+1/2}^L). \quad (3.21)$$

This defines an EM flow map for the stochastic Burgers equation. The notion of monotonicity is that the EM numerical flow map is a monotonically nondecreasing function of quadrature point evaluations, and the slope limiting enforces a specific discrete local maximum principle. More specifically, the numerical method can be decomposed into 4 separate 3-point HHLK monotone schemes at each flux-contributing quadrature point. This is done by decomposing the cell mean value into 4 edge-defined points using its linear subcell representation, for example, the right edge takes the following form

$$H_{i+1/2} = \frac{1}{4} q_{i+1/2}^R - \Delta t F_{i+1/2}(q_{i+1/2}^L, q_{i+1/2}^R) \quad (3.22)$$

$$F_{i+1/2}(q_{i+1/2}^L, q_{i+1/2}^R) = 1/2 \left(\mathbb{F}(q^L, a) + \mathbb{F}(q^R, a) - \alpha(q^R - q^L) \right) \quad (3.23)$$

where α is a yet to be defined constant. The numerical flux is monotone in the sense $\partial_{q^L} F_{i+1/2} \geq 0$, $\partial_{q^R} F_{i+1/2} \leq 0$ if one then defined α to be as eq. (3.20). Therefore, the three-point scheme $H_{i+1/2}$ is monotonically increasing in terms of quadrature points $\frac{\partial H}{\partial q^R}, \frac{\partial H}{\partial q^L} \geq 0$. Therefore the Euler Maruyama scheme is a monotone function of the quadrature point evaluations. If the $N^2(K) \cup N(K)$ -Limiter is employed, the quadrature points themselves are bounded in terms of locally defined cell mean values in such a way one has the resulting local maximum principle of the resulting scheme

$$\bar{u}_{i,j}^{n+1} \in \left[\min_{i,j \in S_{ij}} \bar{u}_{i,j}^n, \max_{i,j \in S_{ij}} \bar{u}_{i,j}^n \right] \quad (3.24)$$

where for a 2D Cartesian mesh one has the set of face-sharing neighbours and their corresponding face-sharing neighbours describes a 13-point stencil. The SSP22 time integration turns this into a slightly wider different local maximum principle (as elaborated on in the appendix of [60]), required when establishing internal local maximum principles for the substages.

The numerical method described above is not proven to be convergent or even claimed to be sensible for this equation, the method proposed simply remains range-bounded, in the sense

$$\bar{u}_{i,j}^{n+1} \in \left[\min_{i,j} \bar{u}_{i,j}^n, \max_{i,j} \bar{u}_{i,j}^n \right]. \quad (3.25)$$

Nevertheless, we wish to demonstrate that the solution will be bounded, provided SSP integration, limiting and Bounded increments are used, and wish to investigate when these conditions are individually violated. To demonstrate this we consider the following cases.

1. SSP22 + Limiter + Bounded increments.

2. SSP22 + Limiter + Unbounded increments.
3. NON SSP integration + Limiter + Bounded increments.
4. SSP22 + Unlimited + Bounded increments.

Case one is theoretically monotone. In case two, the unbounded increments could produce a timestep larger than the radius of monotonicity. In case three a non-SSP integration method has no theoretical guarantees of monotone behaviour. In case 4 without nonlinear limiting strategies, the underlying numerical method is not guaranteed to be monotone.

The numerical setup has the following parameters. We use mesh resolution $n_x = 128, n_y = 128, n_t = 512$, on the space time interval $[0, 1] \times [0, 1] \times [0, 1/2]$. We use a small stochastic basis of noise given by $(a, b) = 1/256(1, 1)$. We use the discontinuous square initial condition given by

$$q_0 = \begin{cases} 1, & \text{where } (x, y) \in [0.1, 0.6] \times [0.1, 0.6], \\ 0, & \text{else.} \end{cases} \quad (3.26)$$

For the unbounded increments, we use the increments $\Delta W \sim N(0, \Delta t)$. For the bounded increments we use the two-point bounded increments from eq. (2.45). For the timestepper, we use SSP22 method 3.1 with a radius of monotonicity 1 or the RK2 method with no radius of monotonicity. For the limiter, we use the $N^2(K) \cup N(K)$ -limiter. We plot the final time solution in fig. 3.1, and we also plot the maximum and minimum as a function of time in fig. 3.1.

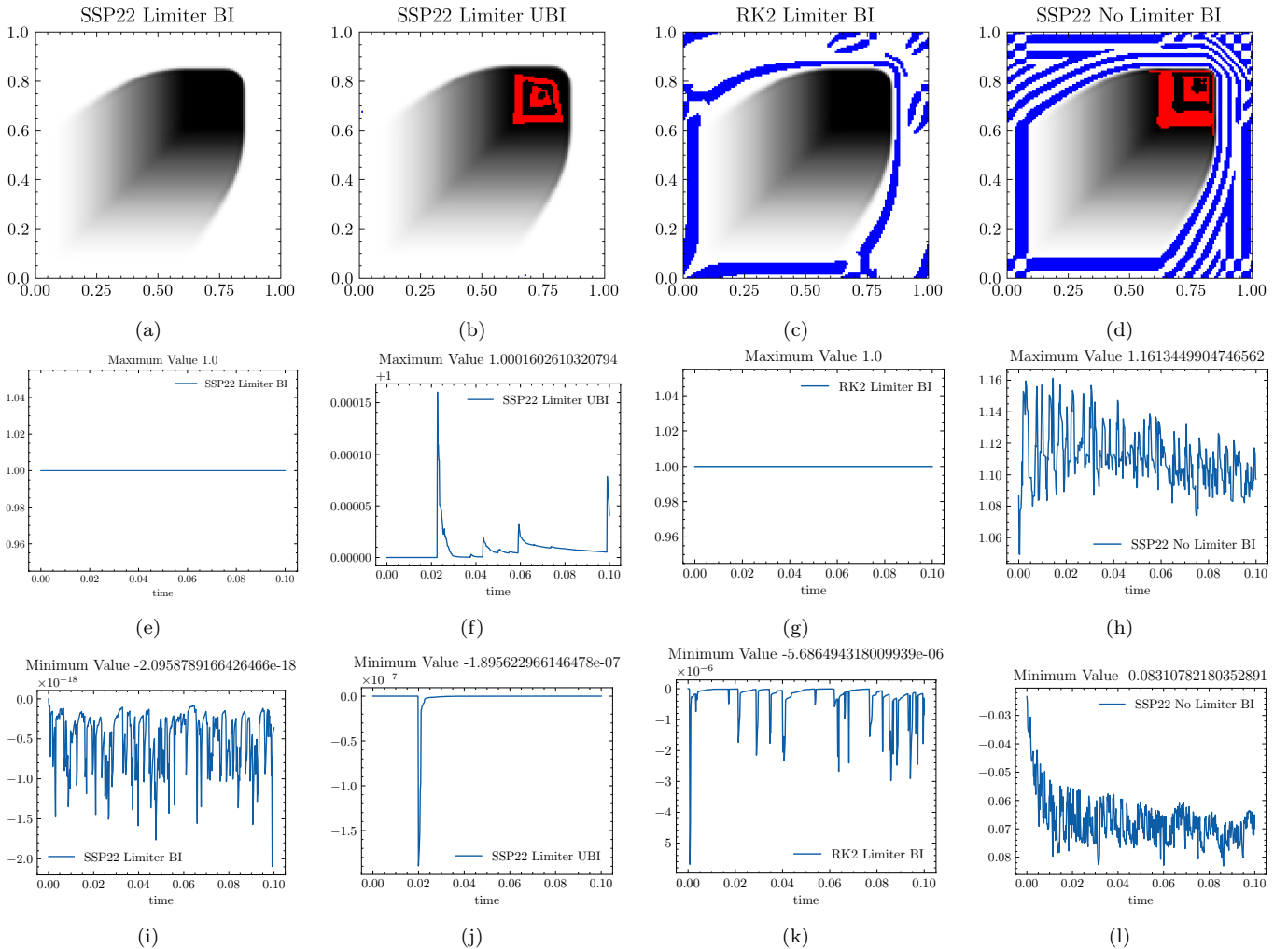


Figure 3.1: We plot the final time plot, of the stochastic Burgers equation in row 1. Red indicates maxima over 1, blue indicates minima under 0 (to machine precision). We plot the maximum value as a function in time, in row 2. We plot the minimum value as a function in time, in row 3. In column 1 we plot the SSP22-Limiter-BI system, in column 2 we plot the SSP-Limiter with unbounded increments. In column 3 we plot the RK2 limited scheme with bounded increments. In column 4 we plot the SSP22 unlimited scheme with bounded increments.

Results of Example 1a. In the first row of fig. 3.1, we plot the final timestep solution of all 4 methods. Where it is observed that SSP time integration, slope limiting and using bounded increments, were all required for a range-bounded numerical solution. In figs. 3.1a, 3.1e and 3.1i we see that SSP22 with limiting and bounded increments makes no global maxima or minima violations over the entire time window. In figs. 3.1f and 3.1j we see that the SSP22 scheme with limiting using unbounded increments generated maxima and minima violations of order 10^{-7} , 10^{-4} respectively. In figs. 3.1g and 3.1k the RK2 Limiter with bounded increments did not generate maxima violations but generated 10^{-6} sized minima violations. The SSP22 scheme with no limiter with bounded increments generated 10^{-1} sized maxima and minima violations. In terms of the magnitude of the monotonicity violations, the absence of a slope limiter produced the largest range boundedness violations, using unbounded increments produced the second largest, and using a non-SSP timestepping method produced the smallest range boundedness violations.

3.2.2. Example 1b: sufficient not necessary

The previous example demonstrates practical merit to each of the three sufficient conditions for monotonic solutions. This example indicates that these conditions may not be strictly necessary in all cases. To demonstrate the practical importance of using a Stochastic SSP method, we follow [35]. The RK method defined as

$$\mathbf{k}^{(1)} = \mathbf{q}^n + a_{12}\Delta t \mathbf{f}(\mathbf{q}^n), \quad (3.27)$$

$$\mathbf{q}^{n+1} = \mathbf{q}^n + b_1\Delta t \mathbf{f}(\mathbf{q}^n) + b_2\Delta t \mathbf{f}(\mathbf{k}^{(1)}), \quad (3.28)$$

is second order when $a_{12} = \frac{1}{2\gamma}$, $b_1 = 1 - \gamma$, $b_2 = \gamma$. Its stochastic extension as a Stratonovich converging Stochastic Runge-Kutta method 2.2 is

$$\mathbf{k}^{(1)} = \mathbf{q}^n + a_{12}\Delta t \mathbf{f}(\mathbf{q}^n) + a_{12}G(\mathbf{q}^n)\Delta \mathbf{S}^n, \quad (3.29)$$

$$\mathbf{q}^{n+1} = \mathbf{q}^n + b_1\Delta t \mathbf{f}(\mathbf{q}^n) + b_1G(\mathbf{q}^n)\Delta \mathbf{S}^n + b_2\Delta t \mathbf{f}(\mathbf{k}^{(1)}) + b_2G(\mathbf{k}^{(1)})\Delta \mathbf{S}^n. \quad (3.30)$$

Dependent on the choice of γ the above scheme has different SSP properties. When $\gamma = 1/2$ the SSP coefficient is $C = 1$ and the scheme is the SSP22 scheme. When $\gamma = -1/40$ the SSP coefficient is $C = 0$, and this particular scheme is often ([21]) used to advocate for the use of SSP methods. For this particular numerical scheme and SPDE, this $\gamma = -1/40$ method blows up entirely. Whilst, this is evidence indicating the merit of SSP time integration over non-SSP integration there may be fairer comparisons. In practice, the $\gamma = -1/40$ scheme is not implemented, it has an unusually large truncation error [35]. We will instead test the schemes when $\gamma = 1/4$, $C = 1/2$, and when $\gamma = 3/4$, $C = 1/2$. These are numerically viable Runge-Kutta methods, in particular when $\gamma = 3/4$ the scheme has the minimum truncation error. We will use bounded increments and limiters such that the SSP22 scheme method is provably monotone, but the $\gamma = 3/4$, $\gamma = 1/4$, are not provably monotone through the SSP property as they are run slightly beyond the radius of monotonicity. The experiment setup is the same as the previous example, and the results are also presented similarly in fig. 3.2.

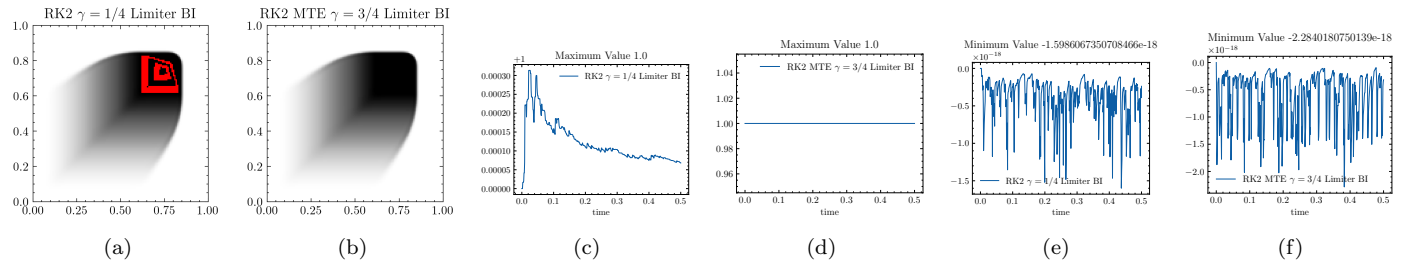


Figure 3.2: In figs. 3.2a and 3.2b we plot the final time solution of the $\gamma = 1/4$, $\gamma = 3/4$ respectively. In figs. 3.2c and 3.2d the maximum value is plotted with time for the $\gamma = 1/4$, $\gamma = 3/4$ respectively.

In figs. 3.1g, 3.1k and 3.2b, one finds that for one particular scheme, in one particular example, running beyond the radius of monotonicity (using a Non-SSP timestepper) was not a strictly necessary condition for the range boundedness preservation in practice. Yet in almost the same setup with a numerical scheme with the same SSP property, the lack of the SSP property in another scheme allowed a non-monotone solution in figs. 3.2d and 3.2f.

Similarly, one could also imagine choosing a particular finite realisation of Brownian motion sufficiently bounded that one does not observe monotonicity violations numerically. Indicating sampling from bounded distributions is not a strictly necessary condition for finite numerical examples.

3.2.3. Example 1c: 2D Advection

In this experiment, we solve the 2D stochastic advection problem

$$dq + \operatorname{div}(\mathbf{u}q)dt + \operatorname{div}(\boldsymbol{\xi}q) \circ dW = 0, \quad q(0, x) = q_0(x) \quad (3.31)$$

at resolution $n_x, n_y, n_t = 128, 128, 512$, on a $[0, 1]^3$ space-time mesh subject to the initial conditions,

$$q_0 = \begin{cases} 1 & \text{for } r_{zal} = \sqrt{(x-0.5)^2 + (y-0.75)^2} \leq 0.15, \quad \text{and } (x \leq 0.475), \\ 1 & \text{for } r_{zal} \leq 0.15, \quad \text{and } (x > 0.525), \\ 1 & \text{for } r_{zal} \leq 0.15, \quad \text{and } (y \geq 0.85), \quad \text{and } (0.475 < x \leq 0.525), \\ (1 - \frac{r_{cone}}{0.15}) & \text{for } (r_{cone} = \sqrt{(x-0.5)^2 + (y-0.25)^2} \leq 0.15), \\ \frac{1}{2}(1 + \cos(\pi \frac{r_{cos}}{0.15})) & \text{for } (r_{cos} = \sqrt{(x-0.25)^2 + (y-0.5)^2} \leq 0.15), \\ 0 & \text{otherwise.} \end{cases} \quad (3.32)$$

specified in [45]. The incompressible vector fields $\mathbf{u}, \boldsymbol{\xi}$ are specified as follows

$$(u^x, u^y) = (-2\pi(y-1/2), 2\pi(x-1/2)), \quad (\xi^x, \xi^y) = \frac{2\pi}{10} (x(x-1)(2y-1), -(2x-1)y(y-1)). \quad (3.33)$$

The deterministic velocity (u^x, u^y) is solid body rotation, and the advection noise (ξ^x, ξ^y) is deformational but incompressible. The solution is theoretically range bounded when using the $N^2(K) \cup N(K)$ -limiter [59] and the SSP104 method 3.3, with the bounded three-point increments described in example 2.2. The diffusion term in the SPDE causes the shape to deform. We plot 16 ensemble members at the final timestep in fig. 3.3, where range boundedness is observed in practice, as is theoretically expected.

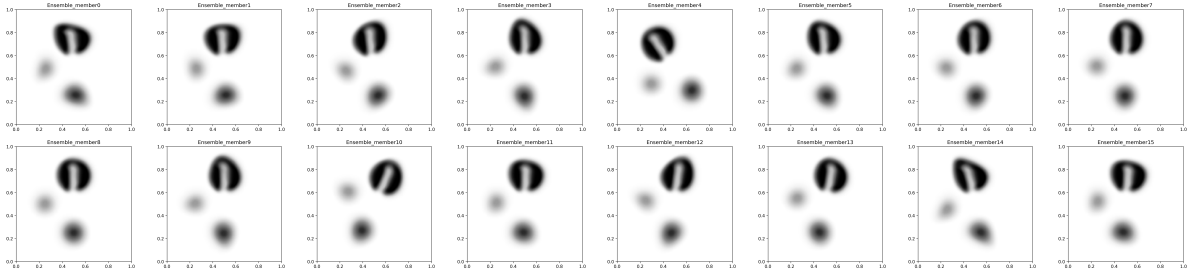


Figure 3.3: We plot 16 ensemble member solutions of the final timestep on a perceptually uniform grey colour scale between $[0, 1]$ undershoots are in blue overshoots are in red (there are no over/undershoots).

3.2.4. Example 1d: Incompressible Euler

In this experiment we solve the incompressible 2D Euler equation, subject to SALT (Stochastic Advection by Lie Transport)-noise [29], the SPDE in vorticity form is given by

$$dq + \operatorname{div}(\mathbf{u}q) + \sum_{p=1}^P \operatorname{div}(\boldsymbol{\xi}_p q) \circ dW^p = 0, \quad q(0, x) = q_0(x), \quad \mathbf{u} = -\nabla^\perp \psi, \quad \psi = -\Delta^{-1} q. \quad (3.34)$$

Where the stream-functions specifying the vector fields $\boldsymbol{\xi}_p = -\nabla^\perp \Psi_p$, are chosen to be

$$\Psi_p(x, y) = 0.0001 \sin(2p\pi x) \sin(2p\pi y), \quad p = \{0, 1, \dots, 7\}. \quad (3.35)$$

Like the deterministic 2D incompressible Euler's equation, this SPDE preserves the local conservation of vorticity and remains bounded in $\|\omega\|_{L^\infty}$, and also possesses a discrete local maximum principle. To numerically locally

preserve the vorticity and maintain a discrete local maximum principle for the EM scheme one can employ a standard C-Grid formulation with one-dimensional slope limiters (for incompressible flow) in [60]. This is described below. We solve the elliptic problem spectrally,

$$\psi_{ij}^n = -\mathcal{F}^{-1} [(k_x^2 + k_y^2)^{-1} \mathcal{F}(q_{ij}^n)], \quad (3.36)$$

where the Nihilist frequency is set manually to account for division by zero, and $2\pi i$ is absorbed into the wavenumber. The value of the streamfunction, is modified as follows $\psi = \psi + \sum_{p=1}^P \Psi_p \Delta \widetilde{W} / \Delta t$. The cell-centered values are then projected to the cell corners

$$\psi_{i+1/2,j+1/2}^n = (\psi_{i,j}^n + \psi_{i,j+1}^n + \psi_{i+1,j}^n + \psi_{i+1,j+1}^n) / 4. \quad (3.37)$$

The normal component of the velocities at faces are computed using a standard C-grid approach

$$(u_{i+1/2,j}^n, v_{i,j+1/2}^n) = \left(-(\psi_{i,j+1/2}^n - \psi_{i,j-1/2}^n) / \Delta y, (\psi_{i+1/2,j}^n - \psi_{i-1/2,j}^n) / \Delta x \right). \quad (3.38)$$

Then one uses the advection algorithm described in [59] for the Euler-Maruyama step, with one-dimensional slope limiters. We employ the differentiable limiter in [59] suitable for incompressible advection. This described Euler Maruyama flow map (with bounded increments) provably has a discrete local maximum principle

$$q_{i,j}^{n+1} \in [m_{i,j}, M_{i,j}], \quad m_{i,j} := \min_{(a,b) \in S_{i,j}} q_{(a,b)}^n, \quad M_{i,j} := \max_{(a,b) \in S_{i,j}} q_{(a,b)}^n, \quad (3.39)$$

where $S_{i,j} = \{(i,j), (i+1,j), (i,j+1), (i-1,j), (i,j-1)\}$ is a 5point stencil. In this test case, we use the Le-Veque initial condition eq. (3.32), and solve for $E = 8$ ensemble members over the space time domain $[0, 1] \times [0, 1] \times [0, 16]$, with periodic boundary conditions. The equation is solved at resolution $512 \times 512 \times 8192$, using the bounded increments in example 2.2 and the SSP33 timestepping method 3.2. The one dimensional slope limiter used is the Differentiable(r) limiter specified in [60], suitable for strictly incompressible flows.

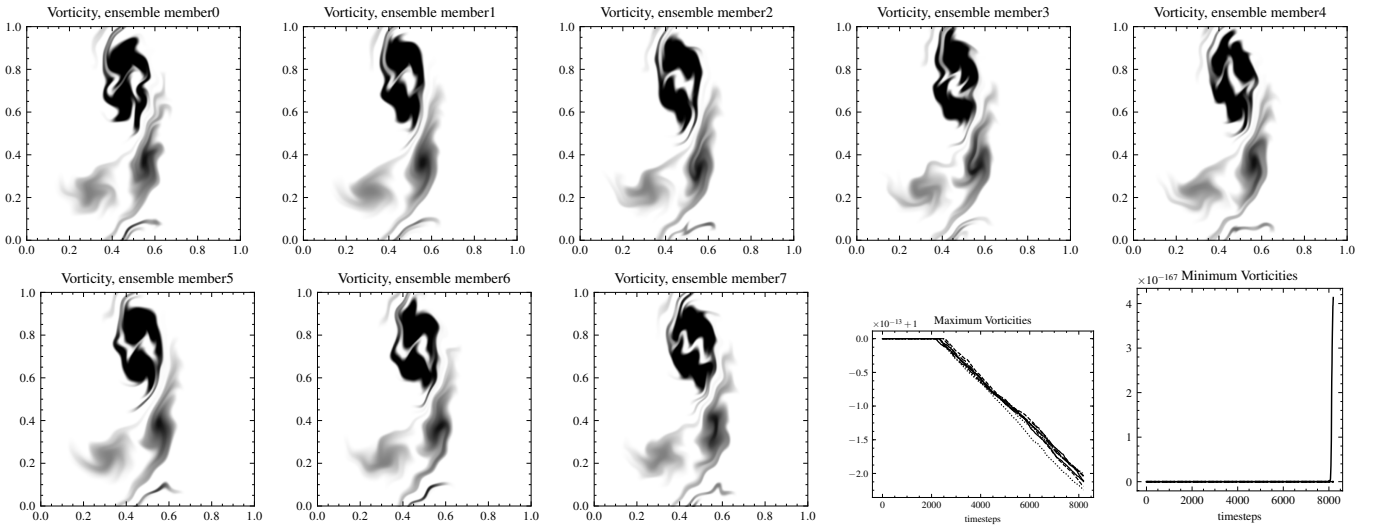


Figure 3.4: Stochastic-2D Euler. We plot 8 ensemble member solutions of the final timestep on a perceptually uniform grey colorscale between $[0,1]$ undershoots are shown in blue and overshoots are shown in red (there are no over/undershoots). Maximums and minima of all ensemble members are plotted and remain bounded.

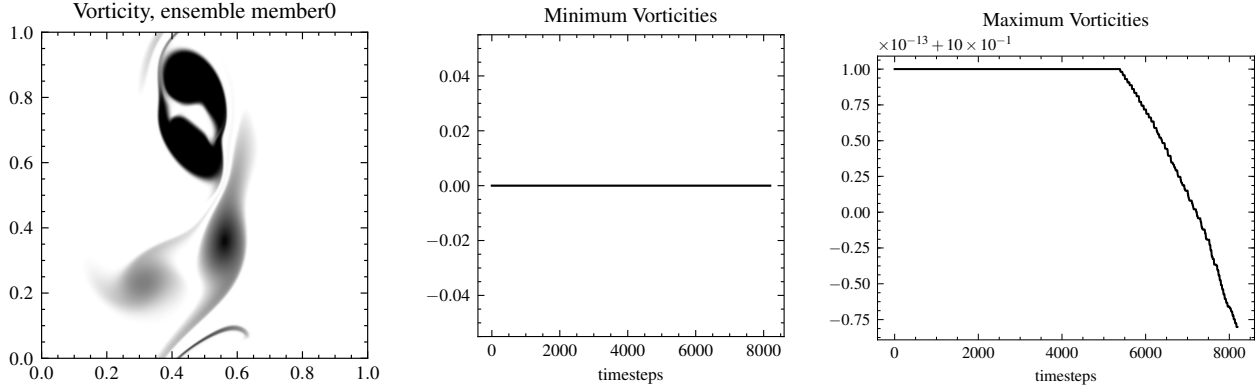


Figure 3.5: Deterministic 2D Euler. We plot a 1 ensemble member solution of the deterministic incompressible Euler equation at the final timestep on a perceptually uniform grey colorscale between $[0,1]$ undershoots are shown in blue overshoots are shown in red (there are no over/undershoots). Maximums and minima are also plotted as a function of timestep.

In fig. 3.5, we plot the solution to deterministic 2D Euler equation, where the slotted cylinder, cone and cosine lump rotate about themselves and one another. In fig. 3.4 we plot 8 ensemble members of the solution to the SALT-2D-Euler equation, the stochastic solutions in fig. 3.4 had additional small-scale dynamics due to the stochastic transport term. In fig. 3.4 and fig. 3.4 all ensemble members remained range-bounded. As expected when using an EM scheme with a probable monotone property, bounded increments and an SSPRK method run below the radius of monotonicity. Such stochastic transport models have been proposed for uncertainty quantification in [29, 9]. However, range boundedness or notions of monotonicity have not been achieved numerically and may be advantageous.

3.2.5. Example 1e: Operator-Splitting GARK

Consider the following Burgers equation with transport type noise,

$$dq_t + \operatorname{div} \left(\frac{1}{2} q^2 \right) dt + \operatorname{div} \left(\sum_{p=1}^P (\xi_p(\mathbf{x}) q) \right) \circ dW_t = 0. \quad (3.40)$$

Designing an approximate Reimann solver suitable for such an SPDE is nontrivial, particularly when the basis of noise $\xi(\mathbf{x})$ varies in space. As a result, it may be difficult to construct a monotone numerical flux function and it may not be possible to prove that the Euler Maruyama scheme has a monotone property. Therefore, we have no monotonicity property for the SSP-SRK method 2.2 to inherit from the EM scheme.

This example demonstrates how one can instead use the SSP-SGARK method 2.4 method and operator splitting to split the problem into sub-problems. Both sub-problems

$$d_t q + f dt = 0, \quad (3.41)$$

$$d_t q + G \circ d\mathbf{W} = 0, \quad (3.42)$$

can be solved with monotonic properties, whereas the combination may not (due to the lack of a well-defined approximate Reimann solver). The nonlinear term

$$f = \operatorname{div} \left(\frac{1}{2} q^2 \right) \quad (3.43)$$

is treated as a deterministic drift and the well-established deterministic Godunov's flux method Appendix A.1 is employed in each spatial direction. Whereas the advection operator

$$G \circ d\mathbf{S}^p = \operatorname{div} \left(\sum_{p=1}^P (\xi_p(\mathbf{x}) q) \right) \circ d\mathbf{S}^p \quad (3.44)$$

will be treated with an established flux form upwind advection algorithm on a C-grid. Then we can apply SGARK or SARK methodology to retain both monotonic properties, without trying to develop a Stochastic approximate Reimann solver as naively attempted previously. The Sequential operator splitting Method 3.4 was used, with $m = 1$, and $n = 4$, the three-point bounded random variable example 2.2 was used for the increments, and the FV2 scheme with $N^2(K) \cup N(K)$ -mp limiter was used for both subproblems. In this setup, we use the initial conditions in eq. (3.32) and use a single incompressible vector field,

$$(\xi_1^x, \xi_2^y) = (2\pi \sin(8\pi x) \cos(8\pi y)/8, 2\pi \cos(8\pi x) \sin(8\pi y)/8) \quad (3.45)$$

which can generate local deformations at a specific length scale. The resolution is $128 \times 128 \times 256$, the space time domain is $[0, 1] \times [0, 1] \times [0, 1/6]$, the boundary conditions are periodic.

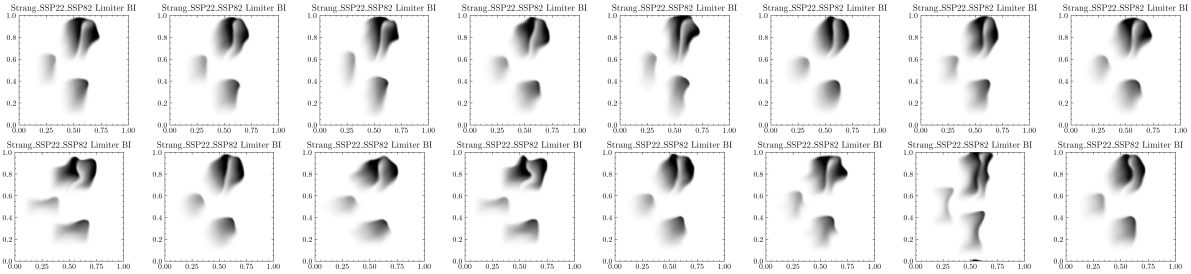


Figure 3.6: Burgers equation with deformational transport noise. We plot 16 ensemble member solutions of the final timestep on a perceptually uniform grey colorscale between $[0,1]$ undershoots are in blue overshoots are in red (there are no over/undershoots).

The result in fig. 3.6 is a range-bounded solution to 2D burgers equation with stochastic transport noise. Demonstrating practical utility for method 2.4, indicating that one can use the ARK or GARK approach to attain a monotonic solution when the EM map may not be provably monotone.

3.3. Numerical demonstrations with data assimilation

The previous examples indicate how SSP methods can be used to generate monotone solutions in various contexts. The next section shall motivate their use, in the context of a simple data assimilation setting. We employ Sequential Importance Sampling (SIS) with resampling, a Sequential Monte Carlo method. We essentially use the bootstrap particle filter of [19], however, we do not use multinomial resampling [12] and instead use the systematic resampling of Kitagawa [37]. We provide an informal introduction to the Bayesian filtering problem for a state space model and the basic particle filter in Appendix A.4 in the interest of being self-contained.

3.3.1. Example 2a: The Twin Experiment, One-dimensional slope limiters

In this example, we test to what extent SSP time integration in combination with monotonic solving strategies, can improve the forecast skill of a stochastic transport model when the reference data is a specific realisation of the same SPDE (solved monotonically). To do so we produce four ensembles,

1. SSP - with monotonic solving strategies - without a particle filter.
2. Without monotonic solving strategies - without a particle filter.
3. SSP - with monotonic solving strategies - with a particle filter.
4. Without monotonic solving strategies - with a particle filter.

We consider the following stochastic compressible transport equation

$$dq(t, x) + (u(t, x)q(t, x))_x dt + \sum_{p=1}^P (\xi_p(x)q(t, x))_x \circ dW_t^p = 0, \quad q(0, x) = q_0(x) \quad (3.46)$$

where $P = 4$, and the compressible vector fields are specified as follows

$$u(x) = \frac{1}{10} (9 + \sin(2\pi x)), \quad \xi_p(x) = \frac{3}{2\pi^2} \frac{1}{p^2} \sin(2\pi p x), \quad p \in \{1, 2, 3, 4\}. \quad (3.47)$$

Subject to the initial condition

$$q_0(x) = \begin{cases} \sin(4\pi x) & \text{where } (x < 0.25), \\ 1 & \text{where } (0.5 < x < 0.8), \\ 0 & \text{else.} \end{cases} \quad (3.48)$$

To solve eq. (3.46) monotonically, we use the noise increments in eq. (2.48), bounded by $A_{\Delta t} = \sqrt{2|\log(\Delta t)|}$, in combination with the SSP33 method 3.2. In space, we use established deterministic monotone methodology. Namely, we let the left and right reconstructed cell face values be specified with a slope limiter

$$q_i^R = q_i^n + 1/2\psi(1/R_i^n)(q_{i+1}^n - q_i^n), \quad q_i^L = q_i^n - 1/2\psi(R_i^n)(q_i^n - q_{i-1}^n), \quad R_i^n = (q_{i+1}^n - q_i^n)/(q_i^n - q_{i-1}^n). \quad (3.49)$$

We define a Euler Maruyama transport velocity $\hat{u}_{i+1/2}$, and use a upwind flux function

$$F_{i+1/2} = F(q_i^R, q_{i+1}^L, \hat{u}_{i+1/2}^n) = \hat{u}_{i+1/2}^+ q_i^R + \hat{u}_{i+1/2}^- q_{i+1}^L, \quad \text{where } \hat{u}_{i+1/2} = u_{i+1/2} + \Delta t^{-1} \sum_{p=1}^P \xi(x_{i+1/2}) \Delta S^p. \quad (3.50)$$

Such that the flux-form Euler Maruyama numerical flow map,

$$q_i^{n+1} = \text{EM} = q_i^n + \frac{\Delta t}{\Delta x} (F_{i+1/2} - F_{i-1/2}), \quad (3.51)$$

is a monotone function of flux contributing quadrature points $(q_i^R, q_{i-1}^R, q_{i+1}^L, q_i^L)$. Conditional on both the slope limiter the quadrature points can be locally bounded. Being a monotone function of locally bounded quadrature point evaluations is an important form of nonlinear stability (see [61, 59, 62, 63]), it implies sign preservation for compressible flow. Sufficient conditions on the slope limiter are $\psi(r) \in [0, \min(2, 2r)]$, we employ the Koren limiter function $\psi(r) = \max(0, \min(1/3 + 2r/3, 2r, 2))$ given in [41].

We recover a reference data set $\{q_{i,ref}^n\}$ with the discrete property $q_{ref}^n \geq 0 \implies q_{ref}^{n+1} \geq 0$, on the space time interval $(x, t) \in [0, 1] \times [0, 128]$, at resolution $n_x, n_t = 64, 1024$. Plotted in fig. 3.7a. We run a $E = 64$ member ensemble on the same space-time window at the same resolution starting from the same initial conditions using the same method and plotted in fig. 3.7a with and without the particle filter. We also run another 64-member ensemble using the third-order unlimited scheme $\psi(r) = 1/3 + 2r/3$, with and without the particle filter, plotted in fig. 3.7b.

Noisy observations occur every $n_{freq} = 8$ timesteps, on the $N_{obs} = 64$ dimensional observation space. The measurement noise is a 64-dimensional normal distribution with standard deviation given by $\sigma = 0.1$. Weights are computed at every $n_{freq} = 8$ timesteps, as is the effective sample size $ESS = (\sum_i w_i^2)^{-1}$. Resampling (by a systematic resampling algorithm [37]) occurs when the effective sample size, falls below $E/2$. This is described in Appendix A.4.

In fig. 3.7a, we plot the solution of the SSP slope-limited ensemble with a particle filter in blue, the ensemble without the particle filter is plotted in red. In fig. 3.7a the reference data is denoted ‘‘Truth’’ and plotted in black. In fig. 3.7a noisy observations are also plotted. In fig. 3.7b we plot the results of the same experiment, but for the unlimited scheme. In the absence of limiting as seen in fig. 3.7b unphysical oscillations and negative values occur, and are not eliminated by the use of a particle filter.

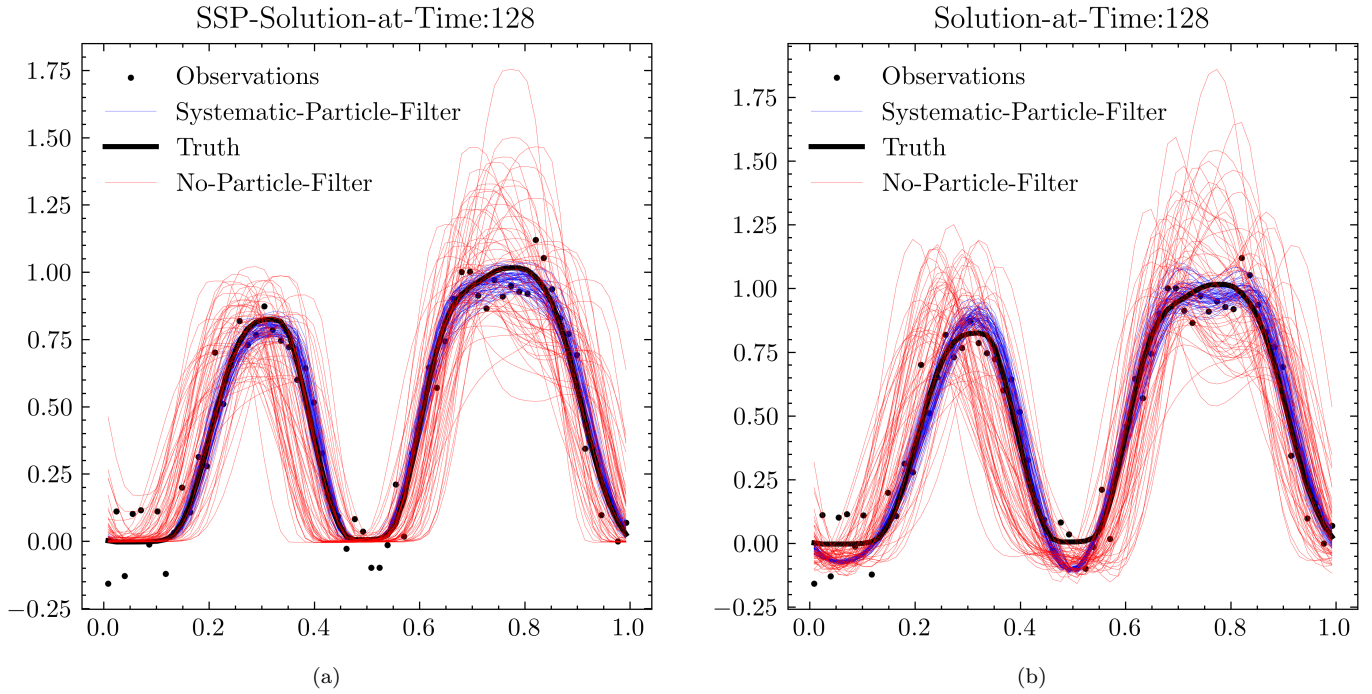


Figure 3.7: Ensemble solutions of eq. (3.46). In fig. 3.7a monotonic solving strategies (SSP-limiting and bounded increments) are employed, in fig. 3.7b the limiting is not used. In black we plot the reference data a realisation of the SSP ensemble, and the noisy observations. In red we plot the ensemble solution without the particle filter, in blue we plot the ensemble solution with the particle filter.

In fig. 3.7a fig. 3.7b the ensembles with the particle filter better tracked the truth by using the noisy measurement data and minimised the variance within the ensembles. Ensemble members in fig. 3.7a, remained positive, and had fewer undershoots and overshoots as compared with the non-monotonic method fig. 3.7b. Whilst systematic resampling drastically improved the forecast capabilities of both ensembles, the systematic errors associated with a non-monotonic solving strategy were still present in fig. 3.7b. Motivating the potential necessity of a monotonic solving strategy.

We quantify some of the ensemble statistics associated with this experiment as a function of lead time. The CRPS is a proper score used to measure the difference between the ensemble and observation cumulative density functions, attained from integrating the Brier skill score over all possible thresholds. A CRPS of 0 indicates accuracy, whereas 1 indicates inaccuracy for additional details regarding CRPS see [1, 17, 18, 22, 47]). In fig. 3.8a we plot the CRPS score for all 4 ensembles. In fig. 3.8b we plot the RMSE score for all 4 ensembles.

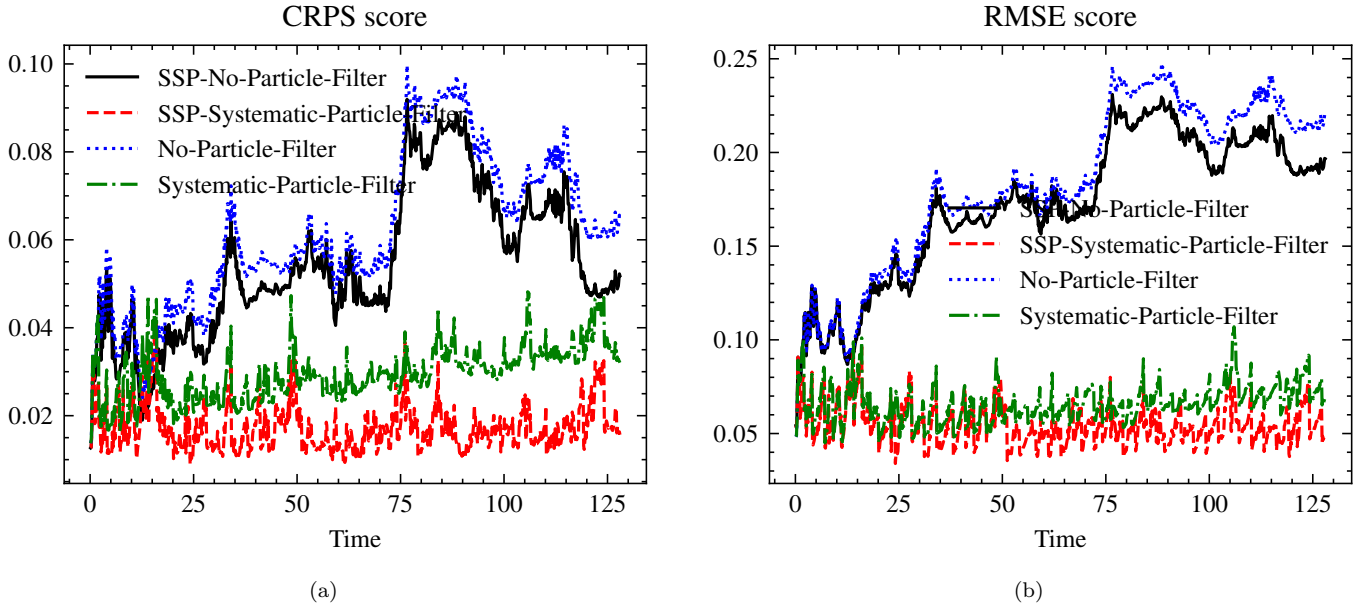


Figure 3.8: In fig. 3.8a and fig. 3.8b, the Continuous Ranked Probability Score and Root Mean Square Error are plotted as a function of lead time respectively. The SSP slope limiting method is plotted with and without a particle filter (systematic resampling) in black and red respectively. The unlimited scheme is plotted with and without a particle filter in green and blue respectively.

The CRPS score was highest (lowest skill score) in the No-Particle-Filter unlimited ensemble, second highest in the SSP-No-Particle-Filter ensemble, third highest in the Systematic-(resampled)-Particle-Filter unlimited ensemble and fourth highest (reaching the most accurate skill score) when using the particle filter with SSP-methodology and limiting. Indicating improved forecast skill from both the monotonic solving strategy and particle filtering.

The use of a particle filter, allowed the ensembles to track the reference data and significantly decreased both RMSE and CRPS, for both SSP and Non-SSP solving strategies. Furthermore, with the particle filter the RMSE and CRPS show evidence of remaining bounded with lead time. Finally, we note that the CRPS score in fig. 3.8a benefited from using both an SSP method with a monotonic solving strategy and a particle filter, producing better results than any other combination. This was also observed in the RMSE, but not so drastically.

3.3.2. Example 2b: One-dimensional slope limiters, Coarse-grained model reduction.

This example is the same as the previous example but we change the reference data. In this example, we test to what extent SSP time integration in combination with monotonic solving strategies, can improve the forecast skill of a model when we define a reference solution, from a high-resolution simulation of the following PDE

$$\frac{d}{dt}q(t, x) + \frac{\partial}{\partial x}(u(t, x)q(t, x)) = 0, \quad q(0, x) = q_0(x), \quad x \in [0, 1], \quad (3.52)$$

a non-linear compressible advection equation with periodic boundary conditions. The velocity $u(x, t) = \frac{1}{10}(9 + \sin(2\pi x))$ is the same compressible vector field as in eq. (3.46). However, the reference data does not come from the ensemble forecast model and differs in both space and time resolution as well as not having stochastic transport terms. We recover a high-resolution reference $\{q_{i,ref}^n\}$ with the discrete property $q_{ref}^n \geq 0 \implies q_{ref}^{n+1} \geq 0$, using the previous numerical strategy. We use $n_x, n_t = 256, 4096$ for the high-resolution data. We have no reason to expect that eq. (3.46) is a reasonable proposal for eq. (3.52), and test whether the particle filter can recover a forecast with skill. We hypothesise that because this reference data has an inherent monotonic property, the ensemble with a similar monotonic property will perform better than the ensemble without this property.

The setup is the same as the previous example however the high-resolution reference data is subsampled in both space and time to produce the same 64-dimensional observation space. Observations can be monotonicity violating. The final time solution of all SSP slope limited ensembles is plotted in fig. 3.9a, and ensembles without limiting are plotted in fig. 3.9b.

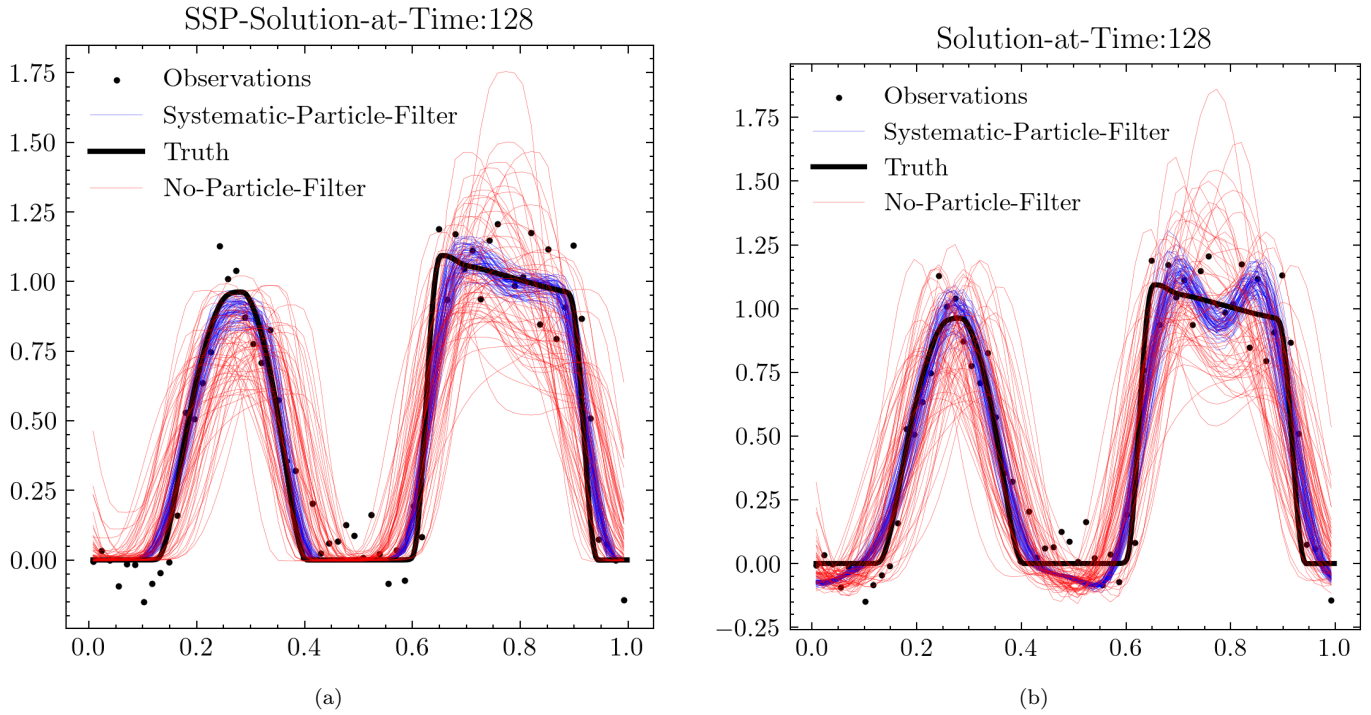


Figure 3.9: Ensemble solutions of eq. (3.46). In fig. 3.9a monotonic solving strategies (SSP-limiting and bounded increments) are employed, in fig. 3.9b the slope limiting is not used. In black we plot the reference data (the solution of a higher resolution PDE), and the noisy observations. In red we plot the ensemble solution without the particle filter, in blue we plot the ensemble solution with the particle filter.

Ensemble members in fig. 3.9a, remained positive, and had fewer undershoots and overshoots as compared with the non-monotonic method in fig. 3.9b, both with and without the particle filter. In fig. 3.9b the particle filter, drew samples from a proposal distribution effected by systematic undershoots and unphysical oscillations, arising from the numerical forward model. Whilst the systematic resampling particle filter drastically improved the forecast capabilities of both ensembles, the systematic errors associated with a non-monotonic solving strategy were still present in the ensemble in fig. 3.9b. In fig. 3.10a we plot the CRPS score for all 4 ensembles as a function of lead time, and in fig. 3.10b we plot the RMSE as a function of lead time.

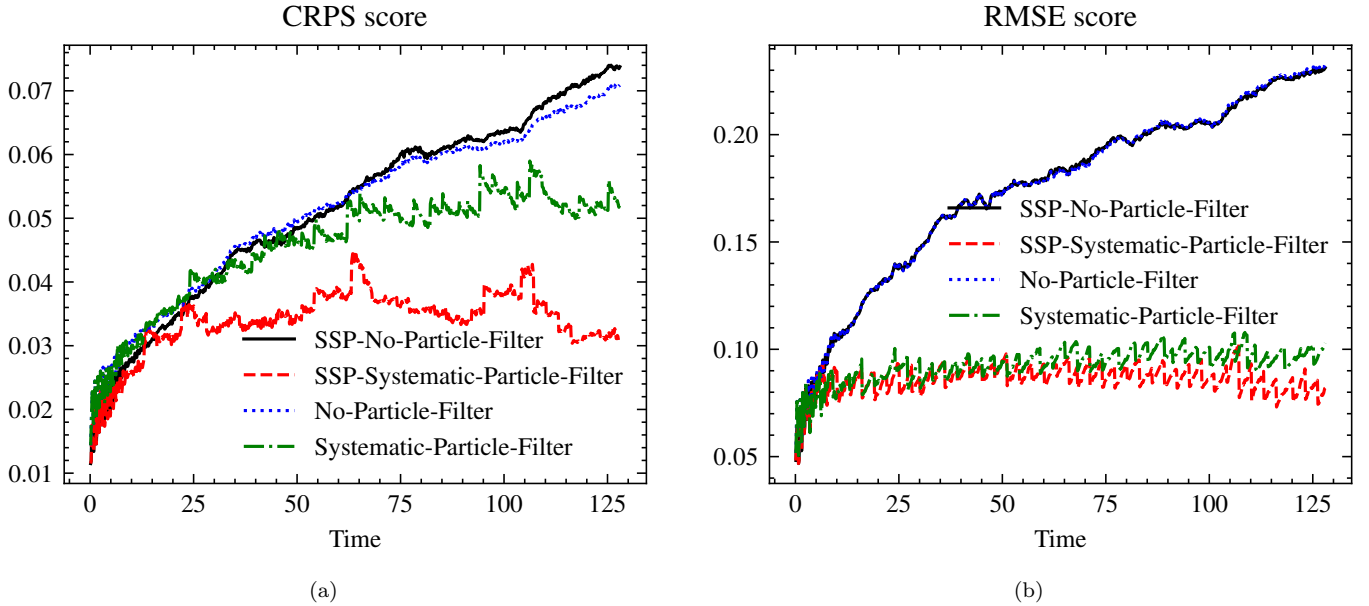


Figure 3.10: In fig. 3.10a and fig. 3.10b, the Continuous Ranked Probability Score and Root Mean Square Error are plotted as a function of lead time respectively. The SSP slope limiting method is plotted with and without a particle filter (systematic resampling) in black and red respectively. The unlimited scheme is plotted with and without a particle filter in blue and green respectively.

In figs. 3.10a and 3.10b without the use of the particle filter both SSP and Non-SSP methods performed similarly in terms of CRPS and RMSE. The use of a particle filter, allowed the ensembles to track the reference data better and significantly decreased both RMSE and CRPS, for both SSP and Non SSP solving strategies figs. 3.10a and 3.10b. Furthermore, the RMSE and CRPS show some evidence of remaining bounded with lead time. Finally, we note that the CRPS score in fig. 3.10a benefited from using the combination of an SSP method monotonic solving strategy and a Particle Filter, producing better results than any other combination. This is also observed to a lesser extent in RMSE in fig. 3.10b. We hypothesise that the increase in CRPS corresponded to the heuristic that an ensemble preserving physically motivated monotonic solutions can better represent latent data arising from a physical process with a similar monotonic property.

4. Conclusion

This work indicates how one can apply deterministic notions of strong stability preservation in the context of stochastic equations. Firstly, monotone solving strategies are required for the solution of the Euler Maruyama map. Secondly, bounded increments are required for the notion of SSP to be understood in the stochastic setting. Thirdly, the deterministic proofs can be directly translated into the stochastic setting upon the appropriate identifications of EM and FE flow maps, allowing a range of SSP RK schemes to be applicable. In the first numerical demonstration in section 3.2.1 we demonstrated the practical utility of all three aspects of the theory when numerically solving a 2D stochastic Burgers equation with constant transport noise. This numerical work required a stochastic extension of the Local-Lax-Friedrich numerical flux, and the use of a local maximum principle limiter in [59]. The second example in section 3.2.2 demonstrated that some of the sufficient conditions for provably monotonic solutions are not always strictly necessary.

In the Additive Runge-Kutta or Generalised Additive Runge-Kutta setting, we showed that one can inherit monotonic properties from an FE scheme and a diffusion-only EM scheme, as opposed to inheriting monotonic properties from the entire EM flow map. In section 3.2.5 we demonstrated that this could be practically used to generate bounded solutions to the 2D Burgers equation with non-constant spatially dependent transport noise. In this example, it was not obvious whether one could create a monotone EM scheme due to the lack of an appropriate Reimann solver, indicating practical utility to the strong stability-preserving stochastic extension to ARK and GARK schemes.

In section 2.4 we remark that stochastic schemes requiring bounded increments can converge weakly or strongly to the solution and be SSP. We prove mean square (strong) convergence order 1/2 of SRK, SARK, methods when using the bounded increments in [49] and we remark how this proof extends to SGARK schemes.

Stochastic SSP methodology can be applied in a wide variety of contexts. Specifically motivating this work are SPDEs describing ocean and climate. In particular, the Stochastic Advection by Lie Transport framework [29] produces SPDEs with nonlinear monotonic properties similar to their deterministic fluid PDE counterparts. In sections 3.2.3 and 3.2.4 it is demonstrated range boundedness and local maximum principles can be numerically attained for the advection equation and 2D incompressible Euler’s equation with transport noise using monotonic solving strategies, bounded increments and an SSP timestepper.

In section 3.3.1 and section 3.3.2 we solve the one-dimensional compressible advection equation with compressible stochastic transport noise. This example tests to what extent SSP methodology (in combination with monotonic solving strategies) can be used to improve ensemble forecast skill both with and without data assimilation (in this case a particle filter). This was tested in an idealised setting when the data was from a realisation of the stochastic forward model and in a non-idealised setting when the data was the realisation of a higher resolution PDE with a monotone property.

We concluded from our experiment and hypothesise more generally that monotonic solving strategies could lead to an increase in forecast skill, should the reference data also arise from a physical process with monotonic properties (such as the positivity of density or temperature). The use of SSP methodology could be conjectured to have more broad applications to SDEs and SPDEs, where positivity preservation, contractive behaviour and other types of nonlinear stability are desirable.

Acknowledgements

JW is especially grateful to R. Hu, for suggesting reading the work of G. N. Milstein, and M. V. Tretyakov. Thankful to A. Lobbe, E. Fausti, and W. Pan for discussions regarding the particle filter. Discussions with D. D. Holm, L. Tianchi, H. Weller, C. Cotter, D. Crisan, O. Street, R. Wood. The corresponding author has been supported during the present work by the European Research Council (ERC) Synergy grant “Stochastic Transport in Upper Ocean Dynamics” (STUOD) – DLV-856408.

References

- [1] S. Arnold, E.-M. Walz, J. Ziegel, and T. Gneiting. Decompositions of the mean continuous ranked probability score. *arXiv preprint arXiv:2311.14122*, 2023.
- [2] M. S. Arulampalam, S. Maskell, N. Gordon, and T. Clapp. A tutorial on particle filters for online nonlinear/non-Gaussian Bayesian tracking. *IEEE Transactions on signal processing*, 50(2):174–188, 2002.
- [3] A. Bain and D. Crisan. *Fundamentals of stochastic filtering*, volume 3. Springer, 2009.
- [4] W.-J. Beyn, E. Isaak, and R. Kruse. Stochastic C-stability and B-consistency of explicit and implicit Milstein-type schemes. *Journal of Scientific Computing*, 70:1042–1077, 2017.
- [5] C. Bolley and M. Crouzeix. Conservation de la positivité lors de la discrétisation des problèmes d’évolution paraboliques. *RAIRO. Analyse numérique*, 12(3):237–245, 1978.
- [6] K. Burrage, P. Burrage, and T. Tian. Numerical methods for strong solutions of stochastic differential equations: an overview. *Proceedings of the Royal Society of London. Series A: Mathematical, Physical and Engineering Sciences*, 460(2041):373–402, 2004.
- [7] N. Chopin. Central limit theorem for sequential Monte Carlo methods and its application to Bayesian inference. 2004.
- [8] S. Conde, S. Gottlieb, Z. J. Grant, and J. N. Shadid. Implicit and implicit–explicit strong stability preserving Runge–Kutta methods with high linear order. *Journal of Scientific Computing*, 73:667–690, 2017.

- [9] C. Cotter, D. Crisan, D. D. Holm, W. Pan, and I. Shevchenko. A particle filter for stochastic advection by lie transport: a case study for the damped and forced incompressible two-dimensional euler equation. *SIAM/ASA Journal on Uncertainty Quantification*, 8(4):1446–1492, 2020.
- [10] D. Crisan and A. Doucet. A survey of convergence results on particle filtering methods for practitioners. *IEEE Transactions on signal processing*, 50(3):736–746, 2002.
- [11] J. Dávila, J. F. n. Bonder, J. D. Rossi, P. Groisman, and M. Sued. Numerical analysis of stochastic differential equations with explosions. *Stochastic Analysis and Applications*, 23(4):809–825, 2005.
- [12] A. Doucet, A. M. Johansen, et al. A tutorial on particle filtering and smoothing: Fifteen years later. *Handbook of nonlinear filtering*, 12(656-704):3, 2009.
- [13] S. Fang, W. Zhao, and T. Zhou. Strong Stability Preserving Multistep Schemes for Forward Backward Stochastic Differential Equations. *Journal of Scientific Computing*, 94(3):53, 2023.
- [14] P. Fearnhead and H. R. Künsch. Particle filters and data assimilation. *Annual Review of Statistics and Its Application*, 5(1):421–449, 2018.
- [15] L. Ferracina and M. Spijker. Step size restrictions for total-variation-boundedness in general Runge–Kutta procedures. *Applied Numerical Mathematics*, 53(2-4):265–279, 2005.
- [16] L. Ferracina and M. N. Spijker. Step size restrictions for the total-variation-diminishing property in general runge–kutta methods. *SIAM journal on numerical analysis*, 42(3):1073–1093, 2004.
- [17] T. Gneiting and A. E. Raftery. Strictly proper scoring rules, prediction, and estimation. *Journal of the American statistical Association*, 102(477):359–378, 2007.
- [18] T. Gneiting and R. Ranjan. Comparing density forecasts using threshold-and quantile-weighted scoring rules. *Journal of Business & Economic Statistics*, 29(3):411–422, 2011.
- [19] N. J. Gordon, D. J. Salmond, and A. F. Smith. Novel approach to nonlinear/non-gaussian bayesian state estimation. In *IEE proceedings F (radar and signal processing)*, volume 140, pages 107–113. IET, 1993.
- [20] S. Gottlieb. On high order strong stability preserving Runge-Kutta and multi step time discretizations. *Journal of scientific computing*, 25:105–128, 2005.
- [21] S. Gottlieb and C.-W. Shu. Total variation diminishing Runge-Kutta schemes. *Mathematics of computation*, 67(221):73–85, 1998.
- [22] H. Hersbach. Decomposition of the continuous ranked probability score for ensemble prediction systems. *Weather and Forecasting*, 15(5):559–570, 2000.
- [23] D. J. Higham, X. Mao, and L. Szpruch. Convergence, non-negativity and stability of a new Milstein scheme with applications to finance. *arXiv preprint arXiv:1204.1647*, 2012.
- [24] I. Higuera. On strong stability preserving time discretization methods. *Journal of Scientific Computing*, 21:193–223, 2004.
- [25] I. Higuera. Representations of Runge–Kutta methods and strong stability preserving methods. *SIAM journal on numerical analysis*, 43(3):924–948, 2005.
- [26] I. Higuera. Strong stability for additive Runge–Kutta methods. *SIAM journal on numerical analysis*, 44(4):1735–1758, 2006.
- [27] I. Higuera, D. I. Ketcheson, and T. A. Kocsis. Optimal monotonicity-preserving perturbations of a given Runge–Kutta method. *Journal of Scientific Computing*, 76:1337–1369, 2018.

- [28] I. Higueras and T. Roldán. New third order low-storage SSP explicit Runge–Kutta methods. *Journal of Scientific Computing*, 79:1882–1906, 2019.
- [29] D. D. Holm. Variational principles for stochastic fluid dynamics. *Proceedings of the Royal Society A: Mathematical, Physical and Engineering Sciences*, 471(2176):20140963, 2015.
- [30] W. Hundsdorfer and M. Spijker. Boundedness and strong stability of runge-kutta methods. *Mathematics of computation*, 80(274):863–886, 2011.
- [31] I. Karatzas and S. Shreve. *Brownian motion and stochastic calculus*, volume 113. springer, 2014.
- [32] C. Kelly, A. Rodkina, and E. M. Rapoo. Adaptive timestepping for pathwise stability and positivity of strongly discretised nonlinear stochastic differential equations. *Journal of Computational and Applied Mathematics*, 334:39–57, 2018.
- [33] D. Ketcheson. An algebraic characterization of strong stability preserving Runge-Kutta schemes. *Undergraduate Thesis, Brigham Young University, Provo, Utah, USA*, 2004.
- [34] D. I. Ketcheson. Highly efficient strong stability-preserving Runge–Kutta methods with low-storage implementations. *SIAM Journal on Scientific Computing*, 30(4):2113–2136, 2008.
- [35] D. I. Ketcheson and A. C. Robinson. On the practical importance of the SSP property for Runge–Kutta time integrators for some common Godunov-type schemes. *International Journal for Numerical Methods in Fluids*, 48(3):271–303, 2005.
- [36] Y. Kiouvrekis and I. S. Stamatiou. Domain preserving and strongly converging explicit scheme for the stochastic SIS epidemic model. *Journal of Computational and Applied Mathematics*, 456:116219, 2025.
- [37] G. Kitagawa. Monte Carlo filter and smoother for non-Gaussian nonlinear state space models. *Journal of computational and graphical statistics*, 5(1):1–25, 1996.
- [38] P. Kloeden and E. Platen. *Numerical Solution of Stochastic Differential Equation*. Berlin; Springer-Verlag, 1992.
- [39] P. E. Kloeden, E. Platen, P. E. Kloeden, and E. Platen. *Stochastic differential equations*. Springer, 1992.
- [40] A. Kong, J. S. Liu, and W. H. Wong. Sequential imputations and Bayesian missing data problems. *Journal of the American statistical association*, 89(425):278–288, 1994.
- [41] B. Koren. *A robust upwind discretization method for advection, diffusion and source terms*, volume 45. Centrum voor Wiskunde en Informatica Amsterdam, 1993.
- [42] J. F. B. M. Kraaijevanger. Contractivity of runge-kutta methods. *BIT Numerical Mathematics*, 31(3):482–528, 1991.
- [43] A. Kurganov and E. Tadmor. New high-resolution central schemes for nonlinear conservation laws and convection–diffusion equations. *Journal of computational physics*, 160(1):241–282, 2000.
- [44] Z. Lei, S. Gan, and Z. Chen. Strong and weak convergence rates of logarithmic transformed truncated EM methods for SDEs with positive solutions. *Journal of Computational and Applied Mathematics*, 419:114758, 2023.
- [45] R. J. Leveque. High-resolution conservative algorithms for advection in incompressible flow. *SIAM Journal on Numerical Analysis*, 33(2):627–665, 1996.
- [46] G. J. Lord, C. E. Powell, and T. Shardlow. *An introduction to computational stochastic PDEs*, volume 50. Cambridge University Press, 2014.

- [47] J. E. Matheson and R. L. Winkler. Scoring rules for continuous probability distributions. *Management science*, 22(10):1087–1096, 1976.
- [48] G. N. Milstein. *Numerical integration of stochastic differential equations*, volume 313. Springer Science & Business Media, 2013.
- [49] G. N. Milstein, Y. M. Repin, and M. V. Tretyakov. Numerical methods for stochastic systems preserving symplectic structure. *SIAM Journal on Numerical Analysis*, 40(4):1583–1604, 2002.
- [50] G. N. Milstein and M. V. Tretyakov. *Stochastic numerics for mathematical physics*, volume 39. Springer, 2004.
- [51] B. Oksendal. *Stochastic differential equations: an introduction with applications*. Springer Science & Business Media, 2013.
- [52] S. Reich and C. Cotter. *Probabilistic forecasting and Bayesian data assimilation*. Cambridge University Press, 2015.
- [53] A. Röbler. Runge–Kutta methods for the strong approximation of solutions of stochastic differential equations. *SIAM Journal on Numerical Analysis*, 48(3):922–952, 2010.
- [54] A. Sandu and M. Günther. A generalized-structure approach to additive Runge–Kutta methods. *SIAM Journal on Numerical Analysis*, 53(1):17–42, 2015.
- [55] C. Scalone. Positivity preserving stochastic θ -methods for selected SDEs. *Applied Numerical Mathematics*, 172:351–358, 2022.
- [56] C.-W. Shu and S. Osher. Efficient implementation of essentially non-oscillatory shock-capturing schemes. *Journal of computational physics*, 77(2):439–471, 1988.
- [57] M. Spijker. Contractivity in the numerical solution of initial value problems. *Numerische Mathematik*, 42:271–290, 1983.
- [58] J. H. Williamson. Low-storage Runge-Kutta schemes. *Journal of computational physics*, 35(1):48–56, 1980.
- [59] J. Woodfield. Higher Order Multidimensional Slope Limiters with Local Maximum Principles. *arXiv preprint arXiv:2407.06437*, 2024.
- [60] J. Woodfield, H. Weller, and C. J. Cotter. New limiter regions for multidimensional flows. *arXiv preprint arXiv:2402.08395*, 2024.
- [61] X. Zhang and C.-W. Shu. On maximum-principle-satisfying high order schemes for scalar conservation laws. *Journal of Computational Physics*, 229(9):3091–3120, 2010.
- [62] X. Zhang and C.-W. Shu. Maximum-principle-satisfying and positivity-preserving high-order schemes for conservation laws: survey and new developments. *Proceedings of the Royal Society A: Mathematical, Physical and Engineering Sciences*, 467(2134):2752–2776, 2011.
- [63] X. Zhang, Y. Xia, and C.-W. Shu. Maximum-principle-satisfying and positivity-preserving high order discontinuous galerkin schemes for conservation laws on triangular meshes. *Journal of Scientific Computing*, 50(1):29–62, 2012.

Appendix A. Appendix

Appendix A.1. Big O notation

We understand the big- $\mathcal{O}(\Delta t)$ -notation in the limit $\Delta t \rightarrow 0$, more specifically, we say $f(\Delta t) = \mathcal{O}(g(\Delta t))$ if there exists a constant $L > 0$ such that $\|f(\Delta t)\|_2 \leq L\|g(\Delta t)\|_2$ for all $\Delta t \in [0, \tau]$ sufficiently small.

Appendix A.2. Multivariate Taylor's theorem

Multivariate Taylor's theorem - Let $f^k : \mathbb{R}^n \rightarrow \mathbb{R}$ be a 1-times continuously differentiable function at the point $\mathbf{q} \in \mathbb{R}^n$. Let $f^k : \mathbb{R}^n \rightarrow \mathbb{R}$ be 2 times continuously differentiable in a closed compact ball around \mathbf{q} , denoted $B_{\mathbf{q}}(r) = \{\mathbf{y} \in \mathbb{R}^n : \|\mathbf{q} - \mathbf{y}\| \leq r\}$ for some $r > 0$. Then for $\mathbf{q} + \mathbf{a} \in B_{\mathbf{q}}(r)$, one has the following Taylors theorem

$$f^k(\mathbf{q} + \mathbf{a}) = f^k(\mathbf{q}) + Df^k|_{\mathbf{q}}\mathbf{a} + R_f^k(\mathbf{q}, \mathbf{a}), \quad \text{where} \quad |R_f^k(\mathbf{q}, \mathbf{a})| \leq L\|\mathbf{a}\|_2^2. \quad (\text{A.1})$$

Then in the vector-valued case, where \mathbf{f} is made of components f^k , one can write down the following component-wise Multivariate Taylor theorem of the following form, with an error estimate on the remainder

$$\mathbf{f}(\mathbf{q} + \mathbf{a}) = \mathbf{f}(\mathbf{q}) + D\mathbf{f}|_{\mathbf{q}}\mathbf{a} + \mathbf{R}_f(\mathbf{q}, \mathbf{a}), \quad \text{where} \quad \|\mathbf{R}_f(\mathbf{q}, \mathbf{a})\|_2 \leq L\|\mathbf{a}\|_2^2. \quad (\text{A.2})$$

Similarly one can write this for the vector \mathbf{g}_p , the p -th component of G .

$$\mathbf{g}_p(\mathbf{q} + \mathbf{a}) = \mathbf{g}_p(\mathbf{q}) + D\mathbf{g}_p|_{\mathbf{q}}(\mathbf{a}) + \mathbf{R}_g(\mathbf{q}, \mathbf{a}), \quad \text{where} \quad \|\mathbf{R}_g(\mathbf{q}, \mathbf{a})\|_2 \leq L\|\mathbf{a}\|_2^2. \quad (\text{A.3})$$

A matrix valued version can be written for G in $\mathbb{R}^{d \times P}$,

$$G(\mathbf{q} + \mathbf{a}) = G(\mathbf{q}) + DG|_{\mathbf{q}}(\mathbf{a}) + \mathbf{R}_G(\mathbf{q}, \mathbf{a}), \quad \text{where} \quad \|\mathbf{R}_G(\mathbf{q}, \mathbf{a})\|_2 \leq L\|\mathbf{a}\|_2^2. \quad (\text{A.4})$$

Appendix A.3. Inequalities

We tabulate some additional estimates on the moments of the bounded normal increments in [49, 50]. All odd moments are zero $\mathbb{E}[(\Delta\tilde{Z})^{2m+1}] = 0, \forall m = \{1, \dots, M\}$. The moment estimate in [49], can be attained by computing

$$\mathbb{E}[(\Delta Z - \Delta\tilde{Z})^2] = \frac{2}{\sqrt{2\pi}} \int_a^\infty (x - a)^2 e^{-x^2/2} dx = \frac{2}{\sqrt{2\pi}} \int_0^\infty y^2 e^{-y^2/2} e^{-ay} dy e^{-a^2/2}, \quad (\text{A.5})$$

Then since $y^2 e^{-y^2/2}, e^{-ay} \geq 0$, one can take the absolute value into the integral and apply holders inequality with the L^∞, L^1 norms on $(0, \infty)$. This allows the following upper-bound

$$\mathbb{E}[(\Delta Z - \Delta\tilde{Z})^2] = e^{-a^2/2} \frac{2}{\sqrt{2\pi}} \int_0^\infty y^2 e^{-y^2/2} e^{-ay} dy \leq e^{-a^2/2} \mathbb{E}[\Delta Z^2] \|e^{-ay}\|_{L^\infty(0, \infty)} = e^{-a^2/2}. \quad (\text{A.6})$$

Similarly, we have that higher-order moments are similarly bounded,

$$\mathbb{E}[(\Delta Z - \Delta\tilde{Z})^{2m}] = \frac{2}{\sqrt{2\pi}} \int_a^\infty (x - a)^{2m} e^{-x^2/2} dx = \frac{2}{\sqrt{2\pi}} \int_0^\infty y^{2m} e^{-y^2/2} e^{-ay} dy e^{-a^2/2} \leq \mathbb{E}[\Delta Z^{2m}] e^{-a^2/2}. \quad (\text{A.7})$$

Taking $a = \sqrt{2k} |\ln(\Delta t)|$, as in eq. (2.48), gives odd moments $\mathbb{E}[(\Delta Z - \Delta\tilde{Z})^{2m+1}] = 0$ and even moments $\mathbb{E}[(\Delta Z - \Delta\tilde{Z})^{2m}] \leq \frac{(2m)! \Delta t^k}{2^m m!}$. Using the Law of Total Expectation, to condition the expectation over $(|x| > a, x < a, x < -a)$, one can compute

$$\mathbb{E}[(\Delta Z^2 - \Delta\tilde{Z}^2)(\Delta Z - \Delta\tilde{Z})] = \frac{1}{\sqrt{2\pi}} \int_a^\infty (x^2 - a^2)(x - a) e^{-x^2/2} dx + \frac{1}{\sqrt{2\pi}} \int_{-\infty}^{-a} (x^2 - a^2)(x + a) e^{-x^2/2} dx \quad (\text{A.8})$$

$$= 0. \quad (\text{A.9})$$

Appendix A.4. Particle filter

This section aims at motivating the particle filter, introducing the Bayesian filtering framework for a state space model, SIS, and resampling, in the interest of this paper being self-contained. The particle filter exposition here is certainly not novel and is considered the most basic available. For a more comprehensive guide see for example, [14, 52, 3, 10, 7] and references therein.

1. Bayesian Filtering Framework In the Bayesian Filtering Framework for a state-space model, the goal is to estimate the hidden state x_k at time t_k , given a sequence of noisy observations $y_{1:k} = \{y_1, y_2, \dots, y_k\}$. The

state transition model $x_k \sim p(x_k|x_{k-1})$ describes how the state evolves. The observation model $y_k \sim p(y_k|x_k)$ describes the likelihood of the observation given the state.

2. Recursive Estimation In a recursive theoretical setting, one supposes that one already has the posterior distribution from the previous time step $p(x_{k-1}|y_{1:k-1})$, and one has access to the transition probability distribution $p(x_k|x_{k-1})$ associated with the forward model advancing from state x_{k-1} , to x_k . The prior distribution $p(x_k | y_{1:k-1})$ could then be theoretically attained by integrating over all possible states for x_{k-1} against the transition probability distribution $p(x_k|x_{k-1})$, as follows

$$p(x_k|y_{1:k-1}) = \int p(x_k|x_{k-1})p(x_{k-1}|y_{1:k-1})dx_{k-1}. \quad (\text{A.10})$$

The state transition probability distribution $p(x_k|x_{k-1})$ accounts for uncertainty associated with the forward model. As one observes the data y_k , one wishes to update the prior distribution into a posterior distribution $p(x_k|y_{1:k})$. This is achieved through the following recursive relationship for the posterior

$$p(x_k|y_{1:k}) = \frac{p(y_k|x_k)p(x_k|y_{1:k-1})}{p(y_k|y_{1:k-1})}. \quad (\text{A.11})$$

This expression is well known and arises from Bayes Rule under the usual assumptions that the hidden state is Markov, and the observations are conditionally independent of the process. $p(y_k|y_{1:k-1})$ is a normalizing constant.

In practice, one cannot perform such an integration, or have access to a transition probability distribution $p(x_k|y_{1:k})$. Instead Monte Carlo (Sequential) Importance Sampling is performed, particles $\{x^{(e)}\}_{e=1}^E$ are drawn from an easier to sample, proposal distribution, denoted q and then associated with an importance weight $\{w^{(e)}\}_{e=1}^E$ according to a likelihood.

3. Sequential Importance Sampling A Monte-Carlo technique called Importance Sampling (IS) can be performed to estimate the properties of hard-to-evaluate distributions. The idea is to draw samples from an easier-to-sample proposal distribution and use importance weights to compensate. However in the non-recursive setting (in the absence of a resampling step) as data becomes available, one would have to recalculate all the importance weights. Instead, if the proposal distribution is assumed to be recursive, importance weights can be updated rather than recalculated. Particle filters are a class of sequential Monte Carlo methods which approximate the posterior distribution $p(x_k|y_{1:k})$ using a set of E weighted Dirac delta functions $\{x_k^{(e)}, w_k^{(e)}\}_{e=1}^E$, as follows,

$$p(x_k|y_{1:k}) \approx \sum_{e=1}^E w_k^{(e)} \delta(x_k - x_k^{(e)}). \quad (\text{A.12})$$

Where δ denotes the Dirac delta function, and $w_k^{(e)}$ denotes the e -th importance weight at time t_k . The importance weight of each particle in the recursive setting can be shown to be [2] updated as follows

$$w_k^{(e)} \propto w_{k-1}^{(e)} \frac{p(y_k|x_k^{(e)})p(x_k^{(e)}|x_{k-1}^{(e)})}{q(x_k^{(e)}|x_{k-1}^{(e)}, y_k)} = w_{k-1}^{(e)} p(y_k|x_k^{(e)}), \quad (\text{A.13})$$

where here in this setting we have assumed that the proposal distribution $q(x_k^{(e)}|x_{k-1}^{(e)}, y_k)$ used to generate new particles is itself the transition model, allowing a cancelling in the denominator and numerator. The probability of observing y_k given the state x_k denoted $p(y_k|x_k)$ is assumed Gaussian so that

$$p(y_k|x_k^{(e)}) \propto \exp\left(-\frac{1}{2}\left(y_k - h\left(x_k^{(e)}\right)\right)^T R^{-1}\left(y_k - h\left(x_k^{(e)}\right)\right)\right), \quad (\text{A.14})$$

where R is the covariance matrix of the observation noise and h is the observation operator. Furthermore, we additionally assumed that R is diagonal with $\sigma^2 I_{m \times m}$, where $\sigma > 0$. So the recalculation of the weights is done

using the following formula

$$w_k^{(e)} = w_{k-1}^{(e)} \exp\left(-\frac{\|y_k - h(x_k^{(e)})\|_2^2}{2\sigma^2}\right). \quad (\text{A.15})$$

4. Resampling Step A resampling step helps to mitigate particle degeneracy, where only a few particles have significant weights. A new set of particles $\{x_k^{(e)}\}_{e=1}^E$ is created by sampling from the current set but with replacement/duplication according to their likelihood weights $\{w_k^{(e)}\}_{e=1}^E$. As suggested in [40] for computational efficiency reasons we resample when particle degeneracy starts to occur, we use the effective sample size diagnostic, given by

$$N_{ess} = \left(\sum_{e=1}^E w_k^{(e)}\right)^{-1}. \quad (\text{A.16})$$

Resampling is done when this falls below a threshold, we choose throughout this work $N_{ess} \leq E/2$. The Systematic resampling algorithm we use is described in [37] and summarised below.

1. Compute vector \mathbf{C} whose j -th component is the cumulative sum of the weights $C_j = \sum_{e=1}^j w^{(e)}$, for all $j \in \{1, \dots, E\}$.
2. Compute vector \mathbf{u} , whose j -th component is $u_j = u + (j - 1)/E$, $j \in \{1, \dots, E\}$ so that \mathbf{u} is made up of equispaced points offset by $u \sim \mathcal{U}(0, 1/E)$. Such that u_j are evenly spaced points in $[0, 1]$.
3. In order to resample we require the indices of the particles corresponding to the positions of \mathbf{u} . More specifically for all elements of \mathbf{u} , we find the indexes of the first position in \mathbf{C} where each value from \mathbf{u} can be inserted without violating the sequential order of the cumulative sum vector \mathbf{C} . In the sense that i is returned such that $C_{i-1} < u_j \leq C_i, \forall j$. This determines which interval and corresponding particles should be resampled according to \mathbf{u} .

As observed data $h(x_k)$ is available we compute weights eq. (A.15), and the ESS eq. (A.16). If eq. (A.16) is less than $E/2$, we compute \mathbf{C} , \mathbf{u} , and then use the “np.searchsorted” function in Python, to generate the indices for the resampling. Subsequently, all weights are renormalised to be $1/E$.

Method Appendix A.1 (Burgers Godunov solver). If one has a 1d edge discontinuity, where q_l, q_r denote the values to the left and right of the discontinuity. Burgers equation has a convex flux function $f(q) = q^2/2$. The solutions are shock solutions if $q_l > q_r$, or a rarefaction fan solution if $q_l < q_r$. This allows one to write down the numerical flux at each cell boundary as

$$F_{i+1/2} = \begin{cases} F_{shock}, & (q_l > q_r), \\ F_{rarefaction}, & (q_l < q_r). \end{cases} \quad (\text{A.17})$$

Where the shock and rarefaction solutions are respectively given by

$$F_{shock} = \begin{cases} f(q_l), & s > 0 \\ f(q_r), & s < 0 \end{cases}, \quad F_{rarefaction} = \begin{cases} f(q_l), & (q_l > 0) \\ 0, & (q_l < 0) \\ f(q_r), & (q_r < 0) \\ 0, & (q_r > 0) \end{cases}, \quad (\text{A.18})$$

here the shock speed s is specified by the Rankine-Hugoniot condition

$$s = \frac{1/2q_l^2 - 1/2q_r^2}{q_l - q_r} = \frac{q_l + q_r}{2}.$$